의학박사 학위논문

Interactome of AMP-activated protein kinase (AMPK)-α1 and -β1 in INS-1 pancreatic beta-cells

INS-1 췌장베타세포 내 AMP-activated protein kinase (AMPK)-α1 및 -β1 단백질의 Interactome 분석

2015년 2월

서울대학교 대학원

의학과 협동과정 종양생물학 전공

문 성 윤

A thesis of the Degree of Doctor of Medicine

Interactome of AMP-activated protein kinase (AMPK)-α1 and -β1 in INS-1 pancreatic beta-cells

By

Sungyoon Moon

February 2015

Division of Cancer Biology

Seoul National University

College of Medicine

ABSTRACT

Sungyoon Moon

Division of Cancer Biology

Seoul National University Graduate School

Introduction: As a heterotrimeric enzyme, AMP-activated protein kinase (AMPK) is a major metabolic sensor in regulating cellular energy homeostasis, and is expressed on many tissues. In particular, AMPK contributes to insulin resistance associated with type 2 diabetes. Generally, cellular processes need tight control of protein kinases, which is influenced by through their formation of complex with other substrates. Despite their crucial function in regulation and pathogenesis, there are limited information on the interaction of protein kinases.

Methods: To identify proteins that interact with AMPK, we performed large-scale affinity purification (AP)-mass spectrometry (MS) of the AMPK-α1 and -β1 subunits. Prior to perform AP-MS, recombinant 6-myc tagged AMPKα1/β1 proteins were transiently transfected in INS-1. Immunoprecipitation was performed accompanied with two different beads: anti-myc antibody-conjugated agarose and magnetic beads. After in-gel trypsin digestion, peptides were analyzed in triplicate by liquid chromatography-tandem mass spectrometry (LC-MS/MS).

Results: Through a large scale analysis using AP-MS approach, we represented that our approach identified 381 unique proteins in the AMPKα1/β1 interactomes: 325 interactors of AMPK-α1 and 243 for AMPK-β1. The result from the magnetic beads capturing shows a higher number of identified

interacting proteins than that from the agarose beads capturing. Furthermore, we identified 196 novel interactors that have not been previously characterized in the existing protein-protein interaction databases. Notably, our bioinformatics analysis suggests that the novel interactors mediated functions that are related to the regulation of actin cytoskeleton. Specifically, several proteins were linked to pancreatic beta-cell functions, including beta-cell development, beta-cell differentiation, glucose-stimulated insulin secretion, and cell-cell communication.

Conclusions: Our AMPK-specific interactome study suggests that our newly identified interactors could be valuable targets for the study of AMPK signaling pathways associated with pancreatic beta cell functions.

* This work is published in *Scientific Reports* Journal.

Keywords: AMP-activated protein kinase (AMPK), affinity purification (AP)-mass spectrometry (MS), pancreatic beta-cell, interactome, proteomics

Student Number: 2009-21863

LIST OF TABLES

LIST OF FIGURES

LIST OF ABBREVIATIONS AND SYMBOLS

AMPK: AMP-activated protein kinase

AP-MS: affinity purification-mass spectrometry

INS-1: rat insulinoma cell line

IP: immunoprecipitation

LTQ: linear ion trap quadrupole

HEK 293: human embryonic kidney 293 cells

RIPA: radioimmunoprecipitation assay

PEI: polyethylenimine

FDR: false discovery rate

BLAST: basic local alignment search tool

GO: gene ontology

IPI: international protein index

IgG: immunoglobulin

FASP: filter-aided sample preparation

LC-MS/MS: liquid chromatography tandem mass spectrometry

SAINT: significance analysis of interactome

AvgP: average of the probabilities in individual replicates

Iqgap1: IQ motif containing GTPase activating protein 1

Gsn: Gelsolin

Myh9: myosin, heavy chain 9, non-muscle

Rhoa: ras homolog gene family, member A

Rac1: ras-related C3 botulinum toxin substrate 1

Vim: Vimenti

CONTENTS

I. INTRODUCTION

Mammalian adenosine monophosphate-activated protein kinase (AMPK) is a serine-threonine kinase that regulates energy homeostasis at the cellular and whole-body levels[1-3]. AMPK is a heterotrimer that comprises a catalytic α subunit, a scaffolding β subunit, and a regulatory γ subunit[1,2]. Orthologs (α1, α2, β1, β2, γ1, γ2, γ3) of AMPK subunits are found in all eukaryotic species and expressed in many tissues[2], suggesting that the structure and regulation of AMPK are evolutionarily conserved[4].

AMPK is activated by nutrient deficiency and cellular stresses, such as glucose deprivation and hypoxia, which initiate metabolic adaptation programs to preserve cellular energy and maintain viability in various tissues, including skeletal muscle, cardiac muscle, adipose tissue, pancreas, and liver[2,3,5,6]. In general, AMPK activity is regulated through allosteric activation by adenine nucleotides, phosphorylation via upstream kinases[7,8], and inhibition of dephosphorylation by protein phosphatases[9].

After activation, AMPK phosphorylates many substrates that regulate metabolism[10], signaling[11], gene expression[12], and tissue-specific glucose and lipid homeostasis[13]. Based on these functions, AMPK is linked to various metabolic diseases, such as type 2 diabetes, obesity, hormonal disorders, cardiovascular disease, and cancer[2,7]. Drugs that activate AMPK, such as metformin and thiazolidinediones, are mainstays in the treatment of type 2 diabetes, underscoring the importance of targeting the AMPK pathway to control metabolic disorders[2,3,5-8].

Recent evidence suggests that AMPK mediates many functions in pancreatic beta-cells, including glucose-stimulated insulin secretion (GSIS)[14], proliferation[15], and survival[16]. Because pancreatic beta-cells have distinct processes with regard to glucose metabolism and depend heavily on glucose and energy-sensing for their function and survival, the functions of AMPK must be examined in beta-cells, which have been described in liver and skeletal muscle. Further, recent findings have demonstrated that AMPK is a positive and negative regulator of insulin secretion[14]. Based on this duality,

considerable effort is under way to determine the functions of AMPK in pancreatic beta-cells. Yet, how AMPK regulates beta-cell function remains elusive[14].

Protein-protein interactions are crucial in all cellular processes[17,18]. As expected, interactions between AMPK and proteins in its downstream pathway are important for most of its functions[19]. Despite the significance of AMPK in beta-cell functions, the interactions between AMPK and other proteins in beta-cells have not been studied extensively. Thus, identifying target molecules that interact with AMPK is critical to understand the functions that are mediated by AMPK. Also, such information can enhance our understanding of disease mechanisms and provide the basis for more specific therapies.

Mass spectrometry-based proteomics has been implemented to investigate protein interaction in a systematic and relatively unbiased manner[17,18], by virtue of technological advances in mass spectrometry. Specifically, affinity purification, followed by mass spectrometry analysis (AP-MS), has become the preferred method of characterizing protein interactions[20,21].

We performed an extensive study of proteins that interact with AMPK-α1 and -β1, which are more highly expressed in pancreatic beta-cells than AMPK-α2 and β2[15,22]. To identify proteins that interact with these subunits, we performed an affinity purification and spectrometric analysis (AP-MS) using a combination of pulldown assay and direct immunoprecipitation of AMPK-α1 and -β1 in INS-1 beta-cells. After a significance analysis using the SAINT program, our interactome comprised 325 and 243 proteins that interacted with AMPK-α1 and -β1, respectively, 196 (51%) of which were novel interactors.

Next, we performed a functional classification of those interacting proteins. Several proteins were found to be involved in regulating actin organization are linked to pancreatic beta-cell functions including, GSIS, beta-cell development, beta-cell differentiation, and cell-cell communication. We also validated those interacting proteins involved in regulating actin cytoskeletal organization. Our interactome data constitute a substantial amount of new information on AMPK-specific interactions.

II. MATERIALS AND METHODS

2.1. Reagents and materials

HPLC-grade acetonitrile (ACN), HPLC-grade water, HPLC-grade methanol (MeOH), hydrochloric acid (HCl), and sodium chloride (NaCl) were obtained from DUKSAN (Kyungkido, Korea). Acetic acid was purchased from TEDIA (Fairfield, OH, USA). Brilliant Blue G-250 and a Bio-Rad protein assay kit were purchased from Bio-Rad (Hercules, CA, USA), and Complete Protease inhibitor cocktail was purchased from Roche (Mannheim, Germany). Other reagents, including 2-mercaptoethanol (β-ME), ammonium bicarbonate (ABC), ammonium persulfate (APS), EDTA, formic acid, iodoacetamide (IAA), magnesium chloride, MES hydrate, potassium chloride, sodium bisulfite, sodium deoxycholate (SDC), sodium pyrophosphate, trifluoroacetic acid (TFA), and Triton X-100 were purchased from Sigma-Aldrich (St. Louis, MO, USA).

2.2. Cell culture

The INS-1 rat insulinoma cells were grown in RPMI 1640 medium, containing 10% heat-inactivated fetal bovine serum, 100 units/ml antibiotics, 1 mM sodium pyruvate, 10 mM HEPES (pH 7.4), and 50 μM β-ME, at 37℃ in a 5% CO_2 incubator.

HEK293T cells were maintained in Dulbecco's modified Eagle's medium (DMEM) with 10% heat-inactivated fetal bovine serum and antibiotics (100 units/ml penicillin and 100 mg/ml streptomycin).

2.3. Plasmid construction and transient transfection for AP-MS

The full-length coding regions of rattus AMPK-α1 and AMPK-β1 were generated by PCR of first-stand cDNA from total RNA of INS-1 cells. Each construct was cloned into the eukaryotic

pcDNA3.1-6-myc-tagged expression vector (Figure 1A). Information for constructs and primers is shown in Figure 1B. Cloned plasmids were confirmed by sequencing. Plasmids were prepared using the Plasmid Midi kit per the manufacturer's protocol.

The plasmids were transfected into HEK293T cells by PEI method[23,24]. Prior to transfection, 12 μg of plasmid in 2 ml serum-free media were mixed with 36 μl PEI solution (1 μg/μl) and incubated for 15 min at room temperature. The solution was added to $1x10^7$ HEK293T cells in a 150-cm^2 dish. Cells were incubated for 4 hours at 37℃ in a CO_2 incubator. After washing with 10 ml of serum-free media twice to remove excess PEI, the cells were incubated with 20 ml of serum-containing media overnight at 37℃. Transiently transfected cells were washed 3 times with ice-cold PBS and pelleted. The pellets were snap-frozen in liquid nitrogen and stored at -80℃ until used.

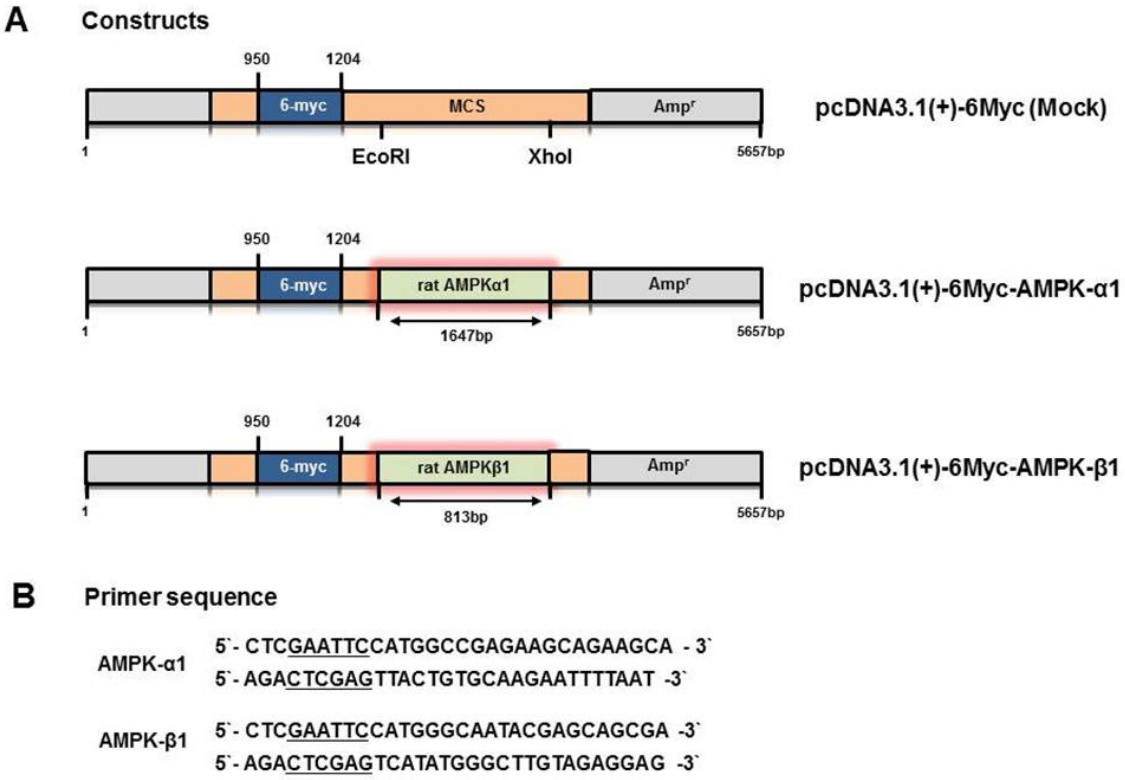

Figure 1. Plasmid DNA construction of AMPK-α1 and AMPK-β1

(A) Schematic of plasmid construction. PcDNA3.1(+)-6Myc-AMPK-α1 and pcDNA3.1(+)-6Myc-AMPK-β1 were generated by inserting DNA fragments containing the entire coding sequences of *Rattus norvegicus* AMPK-α1 and AMPK-β1 into the *EcoRI-XhoI* sites of pcDNA3.1(+)-6Myc. (B) The primer pairs used in each construction.

2.4. Preparation of cell lysates

HEK293T and INS-1 cells were lysed in 200 μl modified RIPA buffer, comprising 150 mM NaCl, 50 mM Tris-Cl pH 7.4, 1 mM EDTA, 1X protease inhibitor cocktail, 0.1 mM PMSF, 0.1% SDC, and 1% NP-40. Cells were disrupted by sonication and centrifuged at 15,000 rpm for 40 min at 4℃ to remove cell debris. Protein concentration was measured by BCA assay. Anti-myc western blot analysis was used to monitor recombinant myc-AMPK expression.

2.5. Pulldown assay using anti-myc coupled to agarose beads

Prior to immunopurification, 1 mg of HEK293T and INS-1 cell lysates were precleared using normal IgG-agarose at a ratio of 200:1 (cell lysate to beads) for 4 hr at 4℃ on a rotary device. Next, recombinant 6-myc-tagged AMPK subunits were immobilized from precleared HEK293T cell lysates to anti-myc-conjugated agarose beads at 4℃ for 4 h.

For the pulldown, precleared INS-1 cell lysate was mixed and incubated with immobilized 6-myc-tagged AMPK subunits as bait overnight at 4℃. Immunopurified complexes were washed 3 times with 500 μl RIPA buffer and eluted with 25 μl 0.1 M glycine (pH 2.5) at room temperature for 5 min. In a control experiment, the same purification was performed, with normal IgG-agarose beads in the immobilization step.

2.6. Pulldown assay using anti-myc coupled to magnetic beads

For Dynabead purification, cell lysates were precleared using Protein G Dynabeads. First, 50 μl of protein G Dynabeads was washed with PBS and incubated for 1 h with 5 μg anti-myc at room temperature. After washes with PBS, the beads were incubated with precleared HEK293T lysate for 4 h at 4℃. The beads were then washed with RIPA buffer and mixed with precleared INS-1 cell lysate overnight at 4℃. After nonspecific proteins were washed away, the immunopurified mixtures were incubated with elution buffer (0.1 M citrate pH 2.5) at room temperature for 5 min. In the control

experiment, immunopurification was performed using lysates from mock-transfected HEK293T cells.

2.7. SDS-PAGE separation, in-gel digestion, and desalting

Immunopurified fractions of each IP were suspended in SDS sample buffer and denatured at 95℃ for 5min. After protein separation by 10% Bis-Tris SDS-PAGE and staining with Brilliant Blue G-250, each lane of the gel was excised, cut into 6 slices, and incubated with 500 μl 200 mM ABC and 50% ACN for destaining. The gel slices were then dehydrated and rehydrated with 200 μl 100% ACN and 200 μl of 0.1 M ABC, respectively. Disulfide bonds were reduced with 200 μl 10 mM DTT. Then, the proteins were alkylated with 50 mM IAA for 30 min at RT in the dark.

The gel pieces were dried in a speed vacuum and incubated overnight at 37℃ with sequencing-grade modified trypsin (Promega, Fitchburg, WI, USA) at an enzyme-to-protein ratio of 1:100 (w/w). The resulting peptides were extracted sequentially from the gel slices with 100 μl 40% ACN/50 mM ABC and 100 μl 80% ACN/0.1% TFA by sonication for 15 min at each stage. After all supernatants were combined, the peptides were dried in a speed vacuum.

The dried peptide mixtures were dissolved in 100 μl 0.1% TFA and desalted using homemade C_{18}-StageTips as described previously[25,26]. Briefly, C_{18}-StageTips were prepared by packing POROS 20 R2 material (Applied Biosystems, Foster City, CA, USA) into 200-μl yellow tips on top of C_{18} Empore disk membranes. The C_{18}-StageTips were washed with 100 μl 100% ACN and equilibrated 3 times with 100 μl 0.1% TFA using a syringe. After loading the samples, the C_{18}-StageTips were washed 3 times with 0.1% TFA and eluted with 100 μl of a gradient of elution buffers, containing 0.1% TFA and 40%, 60%, or 80% ACN. All eluates were combined, dried on a speed vacuum, and stored at -80℃ until further analysis.

2.8. Direct Immunoprecipitation (IP)

To identify interactors of AMPK-α1 and AMPK-β1, we performed direct

immunoprecipitation assay using INS-1 cell lysate. After protein G Dynabeads were coated with rabbit monoclonal AMPK-α1 or AMPK-β1 antibody as bait or normal rabbit IgG as negative control, the beads were mixed with 10 mg of precleared INS-1 cell lysate. The immunopurified mixtures were eluted with 0.1 M citrate buffer. One-third of the volumes of the eluate was digested by FASP as described[27]. The resulting peptides were desalted as described above. The remaining 2 volumes were separated by 1-D electrophoresis on 8-15% SDS-PAGE gels and immunoblotted with antibodies of novel interacting partners for validation.

2.9. LC-MS/MS analysis

Peptide mixtures were analyzed on an EASY nano LC (Proxeon, Odense, Denmark), interfaced with an LTQ Velos mass spectrometer (Thermo Electron Corporation, San Jose, CA, USA), as described[26] with some modifications. nano LC was operated in the 2-column system with a trap column (75 μm I.D. × 4 cm) and analytical column (75 μm I.D. x 15 cm) that were packed in-house with C_{18} resin (Magic C_{18}-AQ, 5 μm, 100 Å). Solvent A was 0.1% formic acid and 2% ACN, and solvent B was 0.1% formic acid and 98% ACN. Fifty milliliters of each sample, dissolved in 50 μl solvent A, was injected into the trap column at 5 μl/min. Peptides were eluted with a gradient of 2% to 40% solvent B over 85 min, followed by a gradient of 40% to 90% for 15 min and 90% over 5 min at 500 nl/min.

The ion spray voltage was set to 1.8 kV in the positive ion mode, and the temperature of the heated capillary was 320℃. A cycle of 1 precursor MS survey spectrum (300–2000 m/z) was acquired in the profile mode. MS/MS scans were taken in the linear trap in a data-dependent manner for the 10 most abundant signal precursor MS ions. All CID MS/MS spectra were acquired using the following parameters: 35% normalized collision energy; ion selection threshold of 500 counts; activation Q of 0.25; and activation time of 30 ms. Dynamic exclusion was performed with a repeat count of 1, 30-s repeat duration, exclusion list size of 50, exclusion duration of 60 s, and ±1.5 m/z exclusion mass width. Overall, 3 technical replicates were analyzed for each dataset.

2.10. Data processing

Raw MS files were processed using the Sorcerer-SEQUEST platform[28] as described with some modifications[26]. MS/MS spectra was examined using a target-decoy database search strategy against a concatenated forward/reversed version of the International Protein Index (IPI) rat (v 3.87, 39,925 entries) and human (v 3.87, 91,464 entries) databases, supplemented with the protein sequences of bovine serum albumin, trypsin, and 6-myc-tagged AMPK-α1 and AMPK-β1. The database search parameters were: full enzyme digest using trypsin (After KR/-) with up to 1 missed tryptic cleavage; a parent ion mass tolerance of 2.0 Da (average mass); a fragment ion mass tolerance of 0.8 Da (monoisotopic mass); fixed modification of 57.02 Da on cysteine for carboxyamidomethylation; and variable modifications of 15.99 Da on methionine for oxidation.

The search data for each experimental scheme were merged and validated using Scaffold 4. Collected datasets were filtered, based on peptide probability, protein probability, and SEQUEST scores, to achieve an estimated false discovery rate (FDR) < 1.0%. The filter criteria were as follows: for charge states of 1+, 2+, and 3+, Xcorr scores should be greater than 1.5, 2.5, and 3.5, respectively; deltaCN should be larger than 0.1; peptide probability and protein probability should exceed 0.95; and the minimum number of unique peptides was set to 2.

To identify proteins that interacted specifically with AMPK subunits and to eliminate false interactions from the negative controls, label-free semiquantitation was performed using Scaffold 4, based on spectral counts in pulldown assay sets. Finally, we sorted interacting proteins into 3 categories (rat only, rat and human concurrently, and human only) according to their species affiliation. Only proteins from rat were considered in the data tables, because INS-1 cells were originated from rat.

To increase the reliability of the interactome data, we performed significance analysis of interactome (SAINT), based on spectral counts, as described[29-31]. The probability scores of the bait and prey proteins were calculated as the average of the probabilities in individual replicates (AvgP). Proteins with AvgP ≥0.9 in 1 biological replicate or those were detected in at least 2 of 4 biological replicates

with AvgP ≥0.5 were likely interactors[30,31].

2.11. Bioinformatics analysis

Gene ontology was performed using DAVID Bioinformatics Resource 6.7[32]. Interactors were categorized into cellular compartment, molecular function, and biological process terms. Only enriched GO terms with a *p*-value < 0.05 were selected. Pathway analysis was performed using the KEGG (Kyoto Encyclopedia of Genes and Genomes) Pathways database (http://www.genome.jp/kegg/). A protein interaction network was generated using STRING 9.1[33] and visualized with CytoScape[34]. AMPK-specific phosphorylation sites were predicted using GPS2.1[35]. The prediction threshold values for GPS2.1 were set to high (3.081) and medium (2.324). Based on the prediction values, phosphorylation sites were classified as high confidence and medium confidence. Phosphorylation sites with low prediction values constituted the no-prediction group.

2.12. Immunoblot analysis and antibodies

Whole HEK293T and INS-1 cell lysates were prepared from $1x10^7$ cells in 200 μl RIPA buffer. Pulldown assay and direct IP assay were performed using Dynabeads as described above. Control experiments were performed using lysates from mock-transfectedHEK293T cells.

The mixtures were incubated overnight at 4℃ with rotation to capture the immune complex. The beads were pelleted by brief centrifugation and washed 3 times with RIPA buffer. Bound proteins were eluted with 100 μl elution buffer, consisting of 0.1 M citrate. The resultant proteins were separated on an 8% to 15% SDS-PAGE gel and immunoblotted with antibodies against AMPK-α1 and AMPK-β1 (Cell Signal, Boston, MA, USA), MYH9 (sc-47199), IQGAP1 (sc-10792), gelsolin (sc-48769) and RhoA (sc-179) (Santa Cruz Biotechnology, Santa Cruz, CA, USA), Rac1 (05-389) (Millipore, Billerica, MA 01821, USA), and vimentin (M0725) (Dako, Glostrup, Denmark).

III. RESULTS (I)

3. Interactome analysis using AP-MS in mammalian system

3.1. Overall scheme for profiling of AMPK-α1 and -β1 interactomes

To identify the interactomes of AMPK-α1 and AMPK-β1 in pancreatic beta-cells, we implemented a novel workflow, combining pull-down assay, based on tagged protein IP, and various support materials. We had planned to overexpress 6-myc epitope-tagged AMPK-α1 and AMPK-β1 by transfection in INS-1 cells. However, we could not obtain a sufficient amount of myc-tagged proteins to perform the AP-MS, due to the low transfection efficiency in INS-1 cells (Figure 2 and 3A).

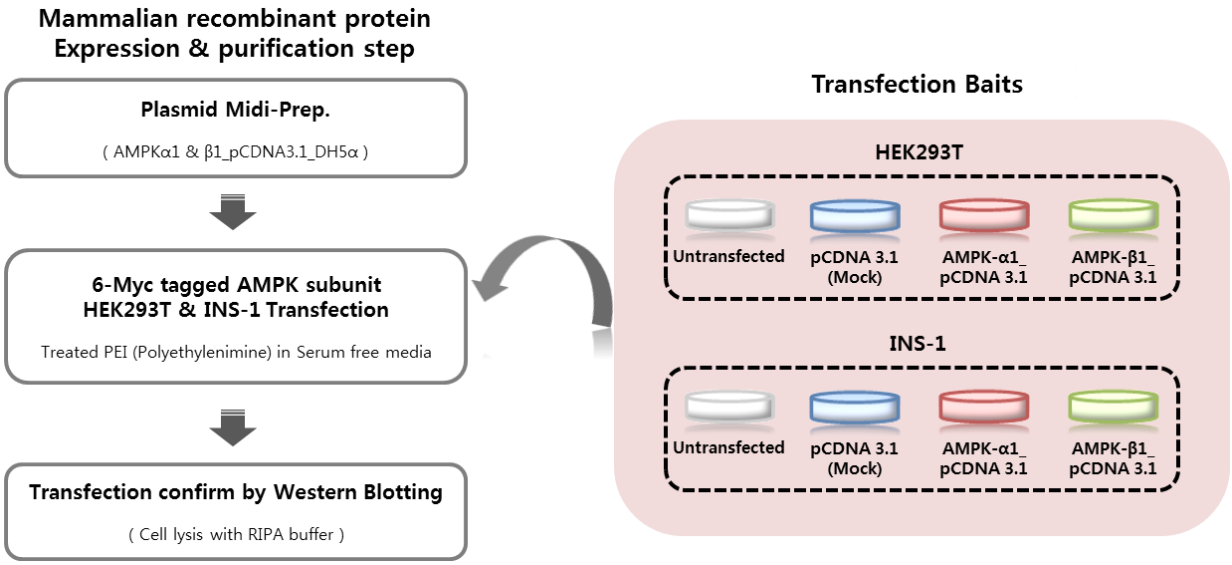

Figure 2. Alternative Transient Transfection in HEK293T

The condition of transient transfection in mammalian expression system was established to increase the expression level of target protein. For expression of recombinant AMPK subunit proteins, HEK293T cells were transfected by PEI with 5ug of plasmid DNA. Myc-tagged AMPK was subcloned into the pCDNA3.1 mammalian expression vector and transfected into HEK293T cell. Lysate from HEK293T cells expressing pcDNA3.1 or Myc-AMPK α1/β1 were immunoblotting with anti-c-Myc antibody.

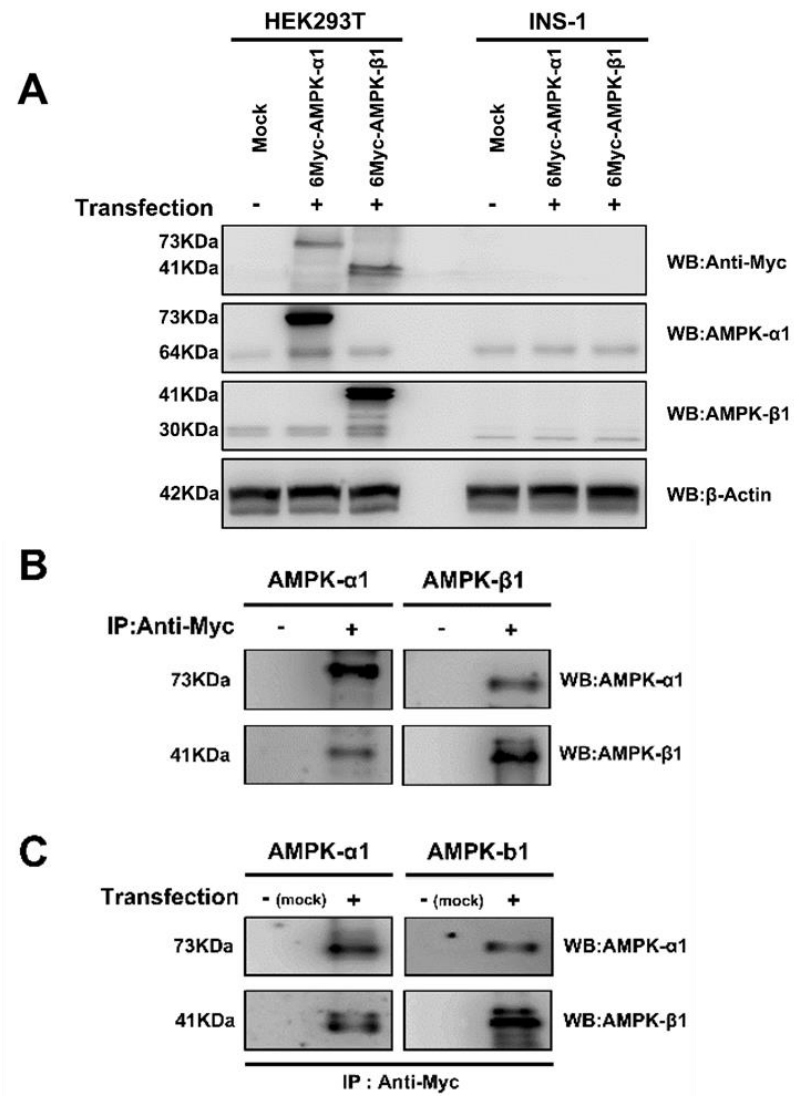

Figure 3. Purification of AMPK subunits in control versus target myc-AMPK IP groups

(A) Lysates from HEK293T cells and INS-1 cells expressing pcDNA3.1 or Myc-AMPK α1/β1 were immunoblotted with anti-c-Myc. Lysate from HEK293T cells expressing pcDNA3.1 or Myc-AMPK α1/β1 was incubated with anti-c-Myc-conjugated agarose (B) or Dynabeads (C) and covalently coupled to matrices for incubation with INS-1 cell lysate. Bound proteins were eluted and subjected to western blot with anti-AMPK-α1 and -β1.

Alternatively, we overexpressed N-terminally 6-myc-tagged rat AMPK-α1 and AMPK-β1 in HEK293T cells and immobilized it to anti-myc–conjugated agarose beads or Dynabeads (Figure 4A, Bait production). Briefly, to express recombinant rat AMPK-α1 and -β1, their full-length cDNAs were subcloned into modified pcDNA3.1 and transfected into HEK293T cells by PEI methods[23,24]. Next, we immobilized the baits using 2 strategies—agarose beads and Dynabeads—to increase coverage of the AMPK interactome.

In the agarose method (Figure 4A), anti-myc- or normal IgG-conjugated agarose beads were incubated with target-transfected HEK293T lysates. Normal IgG-conjugated agarose beads were used as the negative control. For the Dynabeads approach (Figure 4A), we used magnetic beads as IP materials. Anti-myc was also immobilized to Dynabeads. Recombinant AMPK subunits were immobilized using anti-myc-conjugated Dynabeads from transfected HEK293T cells. To prevent any bias from antibody immobilization, anti-myc-conjugated Dynabeads that were incubated with mock-transfected HEK293T lysates were used as bait for the negative control (Figure 4A).

Subsequently, the immobilized 6-myc-tagged AMPK-α1 and -β1 were used as bait in pulldown assays with INS-1 lysates (Figure 4C). To remove nonspecific lysate products, INS-1 lysates were precleared with the same material as in the IP step (Figure 4B)[36]. The proteins that were coprecipitated with myc-tagged baits were separated on a 1-DE 10% bis-tris SDS-PAGE gel and subjected to in-gel trypsin digestion. Finally, the peptide mixtures were desalted using C_{18}-Stagetips[25] and analyzed on an LTQ Velos linear ion trap LC-MS/MS system (Figure 4D). Three technical replicates for each experiment were analyzed. Consequently, we generated 4 datasets of the AMPK interactome (AMPK-α1 agarose, AMPK-α1 Dynabead, AMPK-β1 agarose, and AMPK-β1 Dynabead).

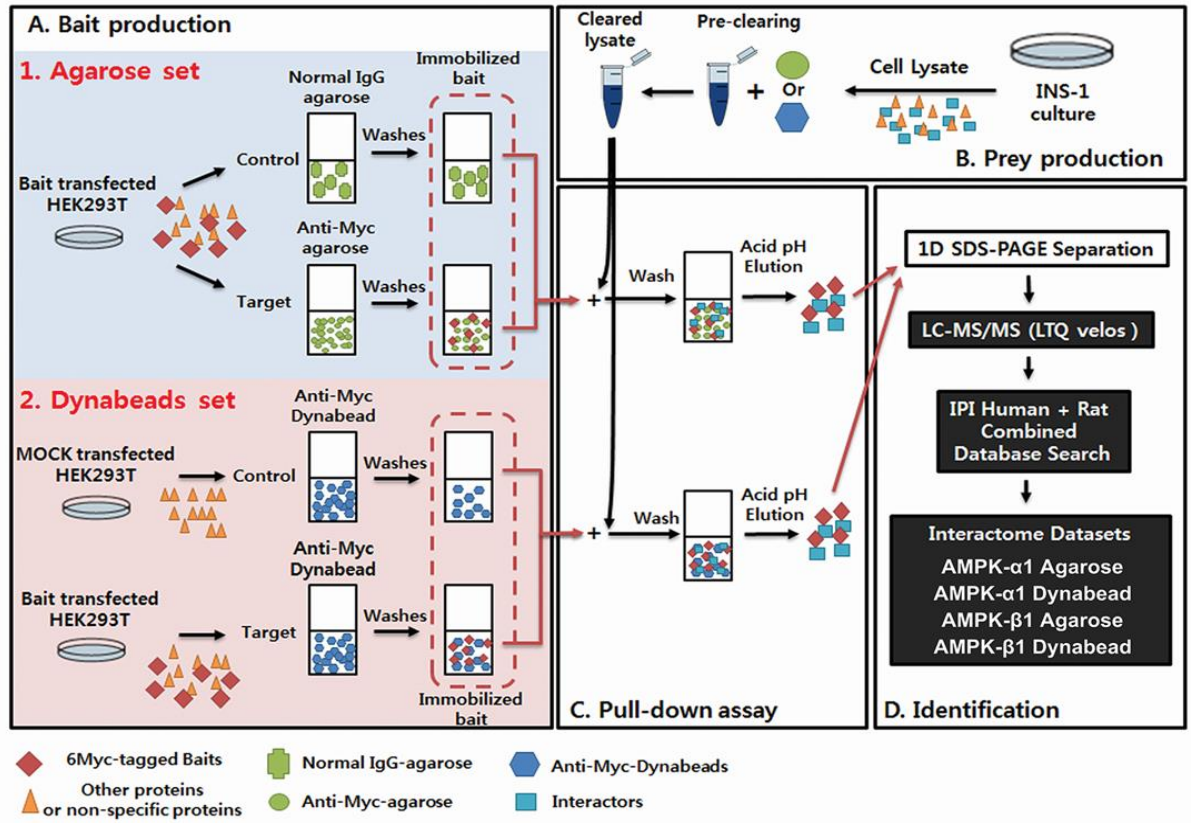

Figure 4. Experimental scheme to examine interactomes of AMPK subunits

The procedure consists of 4 steps in series: A. bait production, B. prey production, C. pulldown assay, and D. identification. To express recombinant 6-myc-tagged AMPK subunits, HEK293T cells were transfected with 5 mg of plasmid DNA by PEI (A). To compare protein interactions we used 2 affinity purification (AP) techniques. In the AP, recombinant myc-AMPK was purified from HEK293T lysates using anti-myc-conjugated agarose beads and Dynabead baits and covalently coupled to matrices for incubation with INS-1 cell lysate (B). The bound Myc-tagged AMPK proteins were immunoprecipitated and separated on a 1-DE 10% Bis-Tris gel and then subjected to in-gel trypsin digestion (C). The digested samples were desalted using homemade stage tips with C_{18} Empore disk membranes. After sample clean-up, the peptides were finally analyzed by LC-MS/MS. A database search was performed on the Sorcerer platform against a concatenated target-decoy database that contained the rat IPI and human IPI databases and their reverse-complements (D). Interacting proteins between the control and target AMPK groups were analyzed using Scaffold 3.

Expression, immobilization, and pull-down were verified by western blot (Figure 3). Overexpression of AMPK-α1 and -β1 in HEK293T cells was confirmed by western blot with anti-myc (Figure 3A). Western blot with AMPK-α1 and -β1 antibodies was also performed to verify the immobilization and coelution of AMPK-α1 and -β1 in the elution fractions of each IP step. As shown in Figure 3B, endogenous AMPK-α1 and -β1 were present in the elution fractions of target baits in the agarose set. In addition, AMPK-α1 and -β1 were detected in the elution fractions of the target baits but not the mock control lane in the Dynabead set (Figure 3C), indicating that both approaches reliably identify interactors of the targets of Interest.

Finally, aliquots of pull-down fractions were loaded onto an SDS-PAGE gel and stained with silver nitrate. Bands that appeared to correspond to AMPK-α1 and -β1 and their interacting partners were observed in the target bait IP (Figures 5A & 5B).

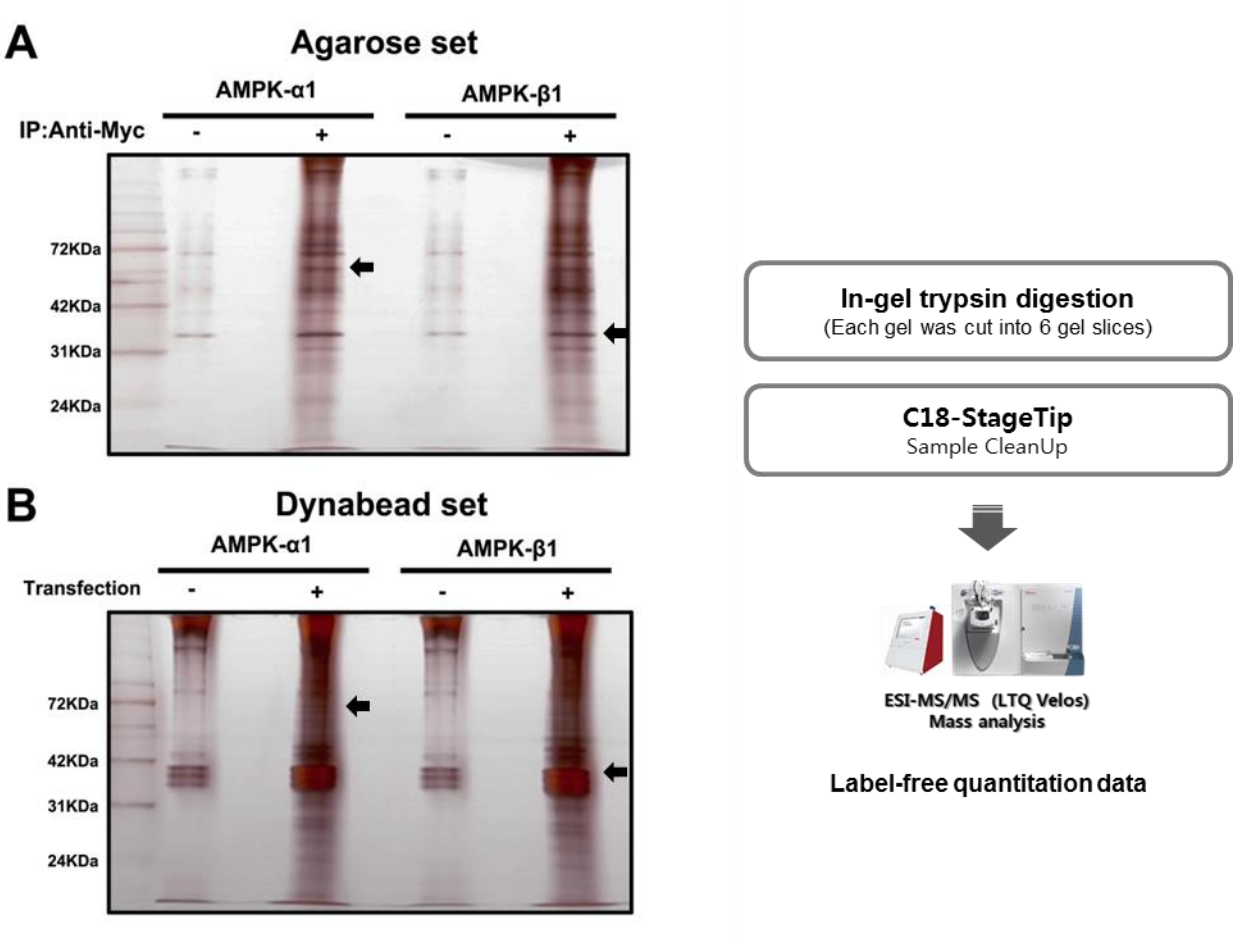

Figure 5. Representative 1D-gel image of affinity purification

In the agarose (A) and Dynabead sets (B), the immunoprecipitates were eluted with citrate buffer and separated on 1D 10% Bis-Tris SDS-PAGE gel. Each gel was cut into 6 gel slices, each of which was subjected to in-gel trypsin digestion.

3.2. Identification and Characterization of AMPK-α1- and –β1- interacting proteins

Recombinant rat AMPK subunits were overexpressed as baits in HEK293T cells, suggesting that some of identified interaction proteins are originated from human. Thus, the proteins that interact with AMPK subunits in INS-1 cells must be classified with regard to species. To separate the interacting proteins that are derived solely from HEK293T cells, MS/MS spectra were searched on the Sorcerer-SEQUEST platform[28] using a target-decoy strategy against a concatenated database that contained the human IPI database (version 3.87, 91,464 entries), rat IPI database (version 3.87, 39,925 entries), and their reverse-complements. The search results were validated and filtered using Scaffold 3 to establish AP-MS datasets at an FDR < 1.0% (Figure 6A).

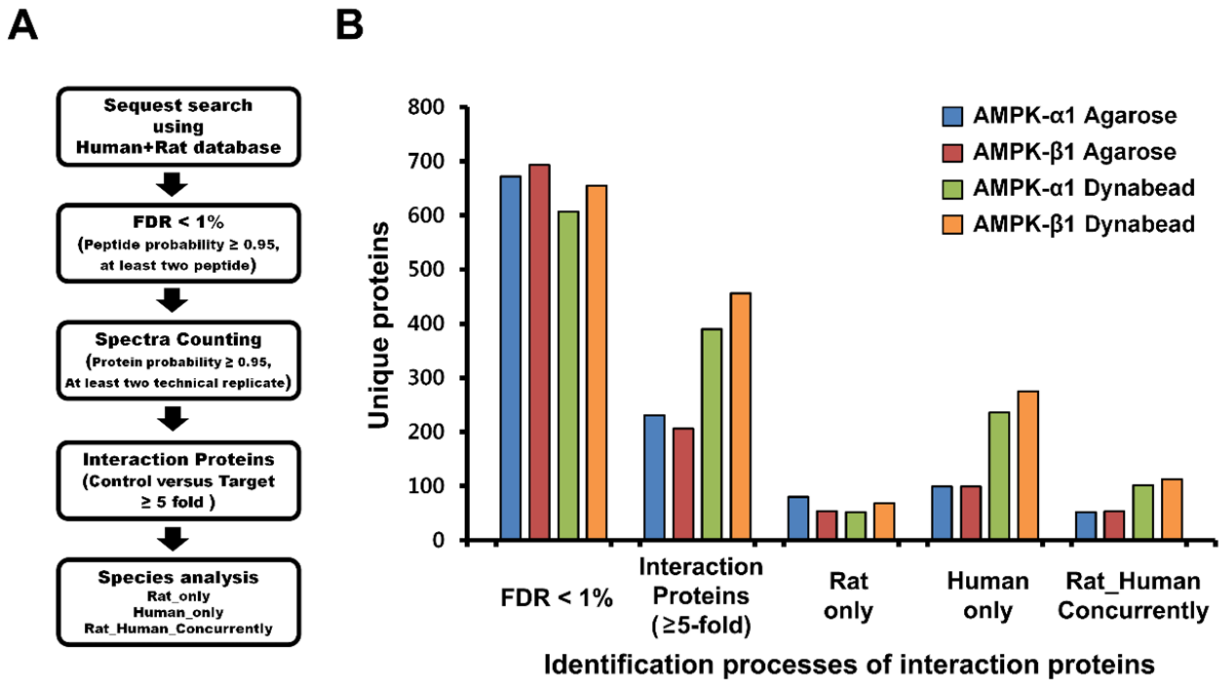

Figure 6. Strategy of label-free quantitation for interactome

To remove nonspecific interactors, we used stringent filtering criteria. (A) Flowchart of semiquantitation for AMPK interactome. (B) Identification of proteins that interact with AMPK-α1 and -b1 subunits. The number of identified proteins is displayed at each filtering stage. AMPK-α1 Agarose, AMPK-b1 Agarose, AMPK-α1 Dynabead, and AMPK-b1 Dynabead are labeled in blue, red, green, and orange, respectively.

Raw data on 63 LC-MS/MS spectra were collected, resulting in 38,286 unique spectra; 17,200 unique peptides, corresponding to 1352 unique proteins, were identified at an FDR of 1%. In experiments in which AMPK-α1 was used as bait, 666 and 601 unique proteins were identified in the agarose and Dynabead set, respectively. In addition, with AMPK-β1 as bait, 687 and 648 unique proteins were identified in the agarose and Dynabead set, respectively (Figures 7A, 7B, and 7C).

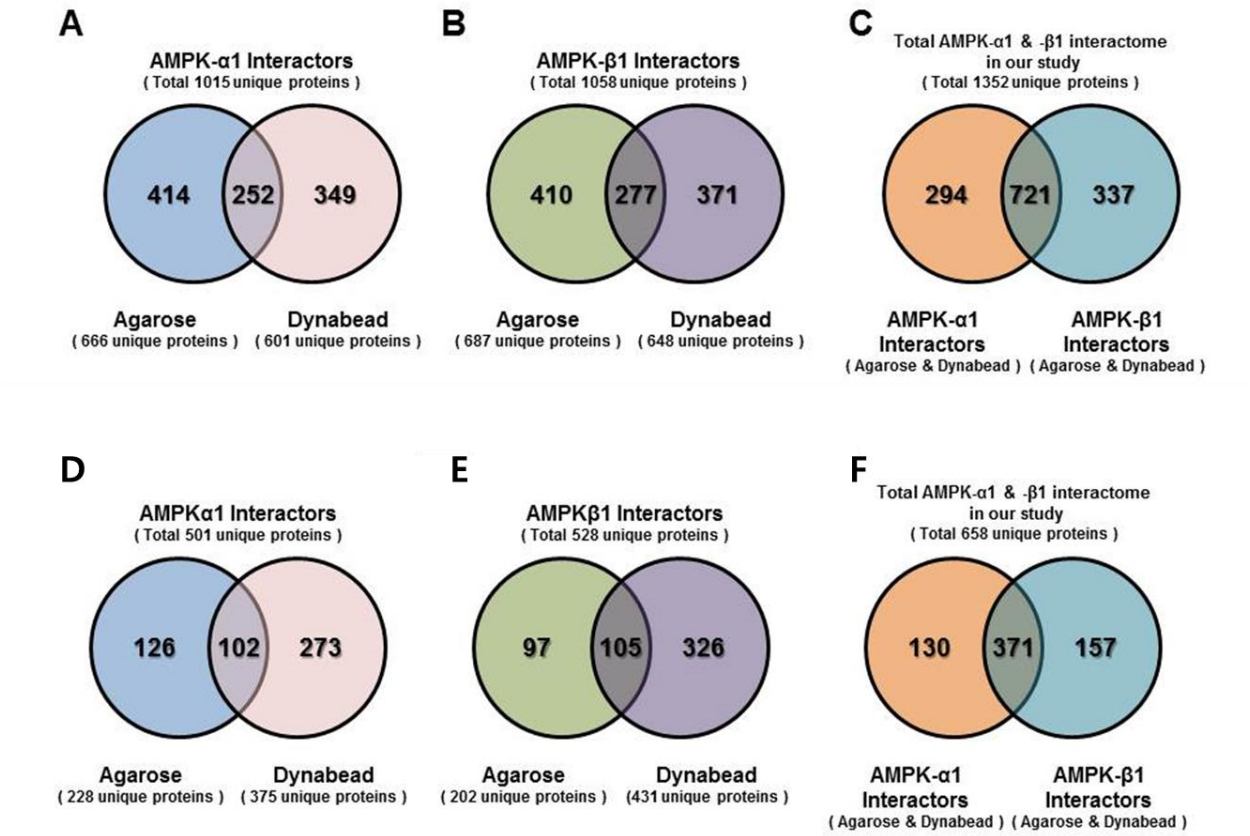

Figure 7. Numbers of proteins identified in each experiment at FDR < 1% and proteins that are quantifiable using stringent criteria

Venn diagrams of the overlap of identified proteins between affinity purification methods for (A) AMPK-α1 and (B) AMPK-β1 and (C) between AMPK-α1 and AMPK-β1 interactors in each experiment at FDR < 1% . (D-F) Venn diagrams of the overlap for semiquantified proteins between the methods of affinity purification for (D) AMPK-α1 and (E) AMPK-β1 and (F) between AMPK-α1 and AMPK-β1. Our 2 approaches using agarose beads and Dynabeads resulted in accumulated coverage of the AMPK-α1 and AMPK-β1 interactome**.**

To distinguish nonspecific interactors, we performed label-free-based semiquantitation using spectral counting[30,37]. In each experiment, unweighted spectral counts of proteins that were identified from the samples that corresponded to the control and baits were exported from Scaffold 3. To include only high-confidence proteins, proteins should be identified at least 2 technical replicates with a protein probability score $\geq$ 0.95 to be input into the semiquantitation. The ratio of the amount of a putative interactor that has coimmunoprecipitated with bait compared with control can be used to examine the specificity of its interaction.

To exclude nonspecific interactors, we used a 5-fold change as the threshold for identifying proteins that interacted with AMPK subunits[38,39]. Because we combined the IPI Human and Rat databases, the IPI accession numbers of the identified proteins were converted into gene names (symbols) and further analyzed. From the 784 proteins that we identified in our interactome, based on IPI accession number, 658 gene symbols were obtained.

With AMPK-α1 as baits, 228 and 375 unique proteins were quantified in the agarose and Dynabead set, respectively, and with AMPK-β1 as bait, 202 and 431 unique proteins were identified, respectively (Figures 7D, 7E, and 7F).

As seen in Figures 8A and 8B, most semiquantified proteins were described by a normal distribution, centered around a ratio of 1 $\log_2$ unit (2-fold), except for proteins that had extreme ratios (1000 and 0.001).

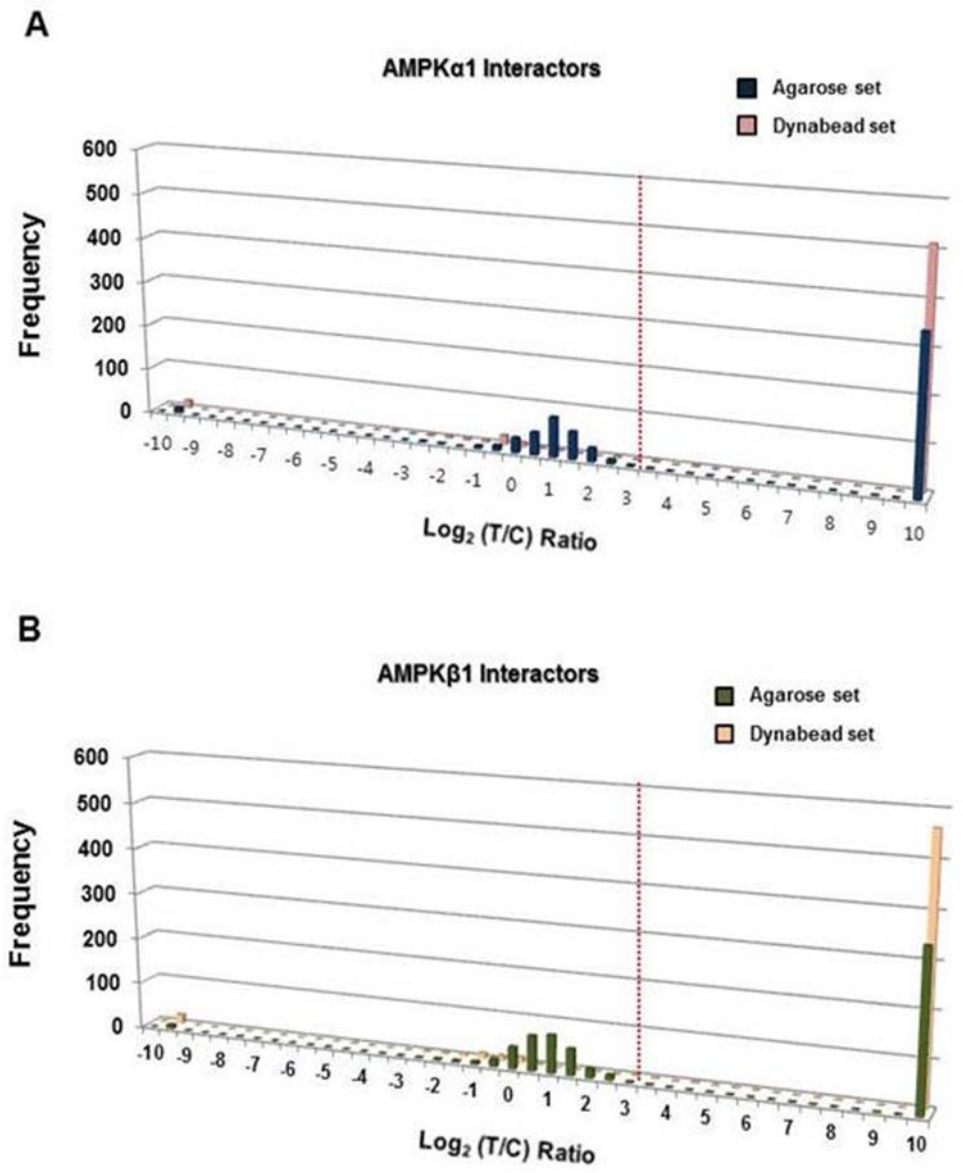

Figure 8. Histograms of log_2 fold-change

(A) The distribution of log_2 ratios (target baits/control baits) of proteins in the AMPK-α1 experiments, including the AMPK-α1 agarose set (blue bar) and AMPK-α1 Dynabead set (pink bar). (B) The distribution of log_2 ratios (target baits/control baits) of proteins in the AMPK-β1 experiments, including the AMPK-β1 agarose set (green bar) and AMPK-β1 Dynabead set (yellow bar). The red lines indicate thresholds of 5-fold change for quantification of proteins interacting with AMPK subunits.

Because AMPK-α1 and -β1 are complexed in cells, we determined whether AMPK subunits were detected in our datasets to assess the reliability of our proteomic approaches. As shown in Figure 9, nearly all AMPK subunits that are expressed in pancreatic beta-cells, such as AMPK-α1, AMPK-α2, AMPK-β1, and AMPK-γ1, were identified with the target baits, whereas the control baits did not contain the spectral counts of AMPK subunits. These results indicate that our immunopurification was reliable.

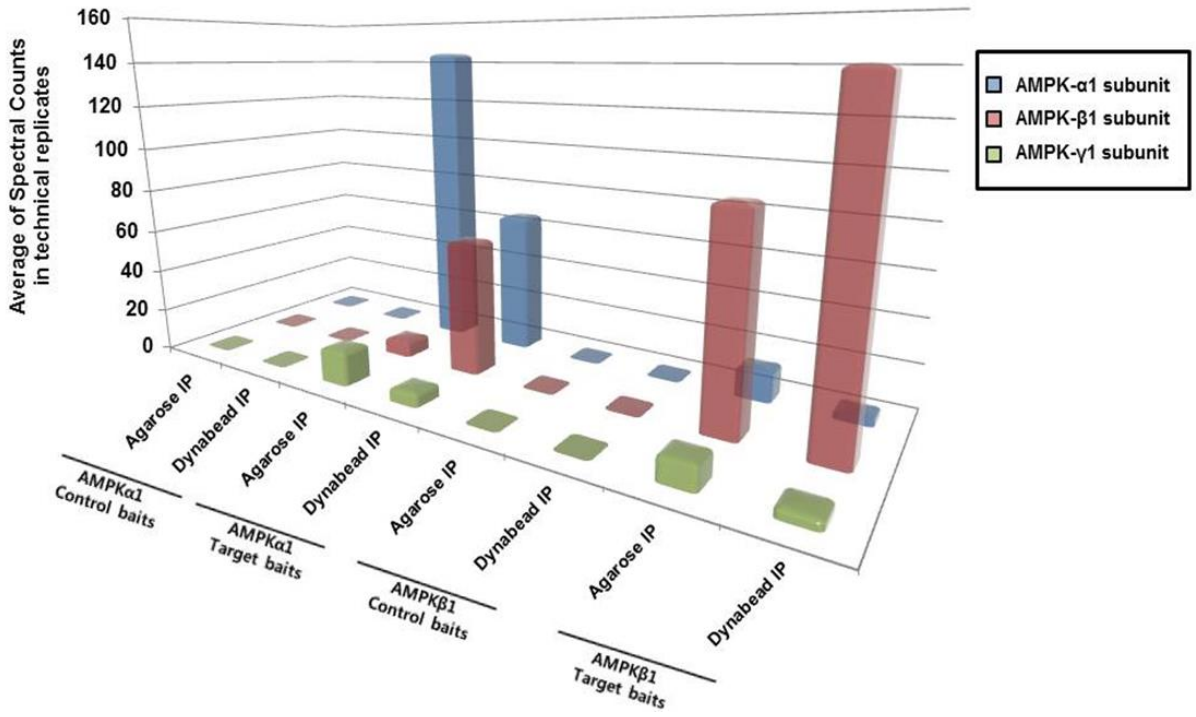

Figure 9. Spectral count distribution of AMPK subunits.

Spectral counts of AMPK-α1 (blue), AMPK-β1 (red), and AMPK-γ1(green) were taken in 3 replicate experiments, which are displayed in bars. Spectral counts were expressed as the average of the spectral counts of 3 technical replicates.

Finally, the amino acid sequences of the filtered proteins were examined with regard to species using the protein grouping algorithm in Scaffold 3 to sort INS-1-specific interactors. In Scaffold 3, proteins that are identified with the same sequence of peptide (called the sharing peptide) are represented as protein groups. Because we used a concatenated human and rat database, we could verify whether the identified proteins were human or rat. For example, if a protein group comprises only rat proteins, it clearly matches rat proteins and not its human orthologous counterpart. However, if a protein group contains a mixture of human and rat proteins, it is derived from HEK293T or INS-1 cells.

The identified proteins were classified into 3 groups: Rat_only, Rat_Human_Concurrently, and Human_only (Figures 10A – 10F). A total of 125 AMPK-α1- and 114 AMPK-β1-specific interactors were identified as 'Rat_Only;' versus 301 AMPK-α1- and 328 AMPK-β1-specific 'Human_Only' proteins. Proteins in the Rat_Human_Concurrently groups that had 99% identities between the rat and human homologs were included in the final list by BLAST analysis. After a homology filtering step, 101 AMPKα1- and 102 AMPKβ1-specific proteins were detected as 'Rat_Human_Concurrently.' Consequently, 231, 390, 206, and 456 proteins were identified as specific interactors in the AMPK-α1 agarose, AMPK-α1 Dynabead, AMPK-β1 agarose, and AMPK-β1 Dynabeadsets, respectively (Table 1 and Figure 6B).

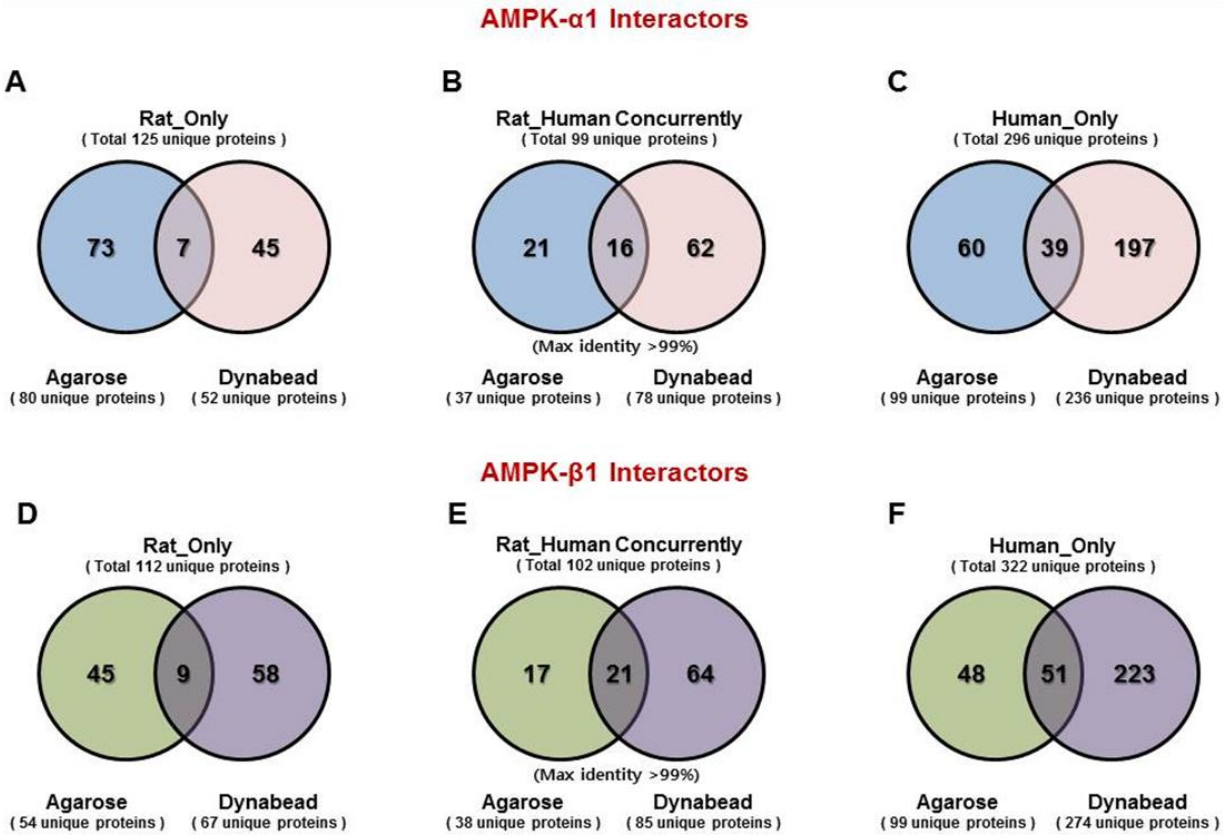

Figure 10. Comparison between numbers of proteins belonging to species affiliation groups

For AMPK-α1-interacting proteins, Venn diagrams show the overlap of proteins between affinity purification methods for Rat_only (A), Rat_Human_Concurrnetly (B), and Human_only groups (C). For AMPK-β1-interacting proteins, Venn diagrams show the overlap of proteins between affinity purification methods for Rat_only (D), Rat_Human_Concurrnetly (E), and Human_only groups (F). Only proteins that had 99% sequence identity between Rat and Human homologs by BLAST analysis were included in the final list of the Rat_Human_Concurrently group.

Table 1. Summary of mass spectrometry analysis

IP Baits	Identifications									Filtered data set FDR<1%, probability>95%, Ratio (T/C)a >5			
	Proteins			Unique Peptides			Unique Spectra			Unique proteins			
	Control baits	Target baits	Total Number of Protein	Control baits	Target baits	Total Number of peptide	Control baits	Target baits	Total Number of Spectra	Rat Only	Rat & Human Concurrently	Human Only	Total Number of Protein
Alpha1 Agarose IP	598	660	666	2608	4166	4585	5041	8230	10792	80	52	99	231
Alpha1 Dynabeads IP	284	598	601	848	3397	3646	1890	6697	7722	52	102	236	390
Beta1 Agarose IP	625	680	687	2950	4222	4746	5609	8315	10980	54	53	99	206
Beta1 Dynabeads IP	292	644	648	838	3966	4223	1857	7743	8792	68	113	275	456

[a] Ratio of target baits versus control baits

3.3. Functional classification of AMPK-specific interactors

To determine the functions of proteins that interact with AMPK subunits in INS-1 cells, the AMPK-α1 and -β1 binding partners were grouped by Gene Ontology (GO) term using the DAVID bioinformatics resource tool as biological process, cellular compartment, and molecular function[32]. To identify the GO categories that were overrepresented in proteins in the Rat_only group compared with the Human_only and Rat_Human_concurrently groups, 502 AMPK-α1 and 529 AMPK-β1 binding partners were individually subjected to GO analysis by affiliation (Figure 11).

Proteins that mediate the organization and regulation of the actin cytoskeleton were significantly enriched in the Rat_only group versus the other groups (Figures 11A and 11B). In addition, a significant proportion of proteins in the Rat_only group had cytoskeletal protein-binding and motor activity. The commonly enriched categories in the 3 groups of species were linked to major pathways that are associated with AMPK, such as metabolism, translation, RNA processing, cell cycle, and gene expression. Also, most proteins were distributed broadly throughout the cytosol, mitochondria, nucleolus, and ribosome.

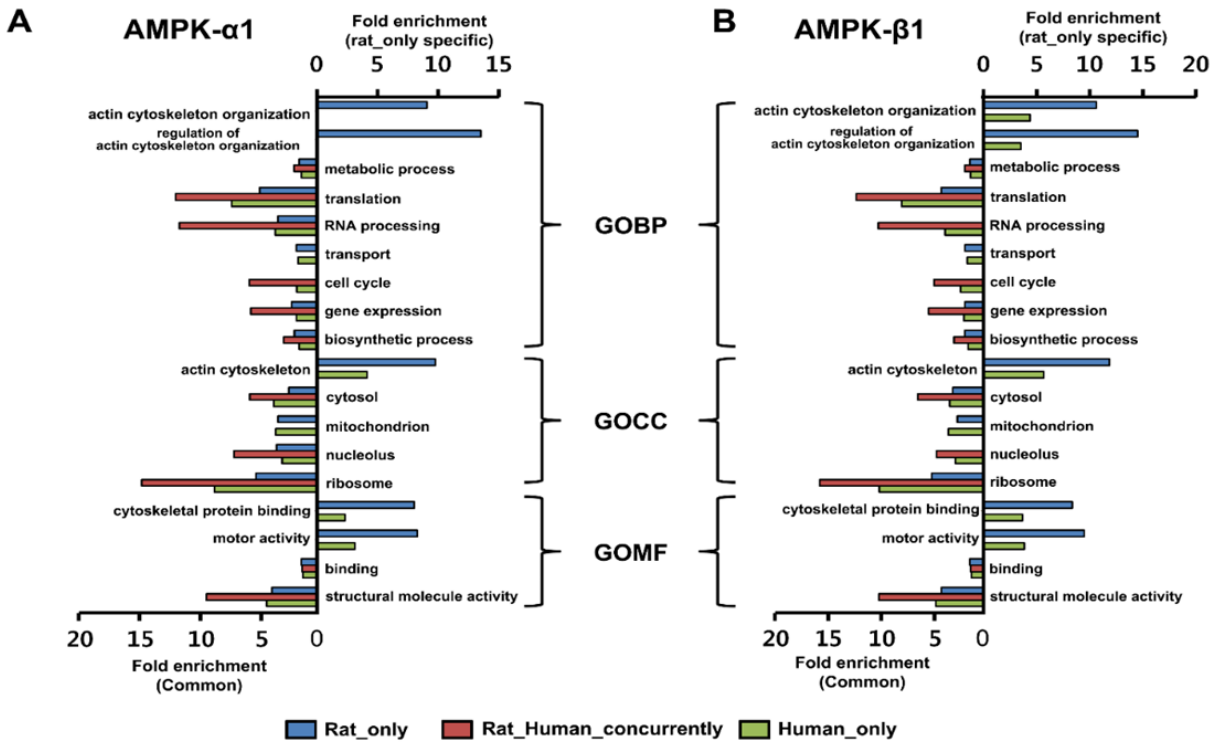

Figure 11. Functional GO annotation of AMPK-α1 and AMPK-β1 interactome

All identified proteins—502 AMPK-α1- and 529 AMPK-β1-interacting proteins—were grouped, based on GO terms. The IPI accession numbers of each set were analyzed using the DAVID server (http://david.abcc.ncifcrf.gov/). GO terms enriched from proteins identified in rat_only were classified as rat_only-specific, whereas those from proteins in both human and rat groups were classified as common. GO term enrichment analysis were performed for rat_only-specific and common species groups. Fold-enrichment for a particular GO term describes the ratio between the numbers of genes belonging to a specific GO term and the total number of genes in the genome with at least 1 GO annotation. Enriched GO terms for biological process (GOBP), cellular component (GOCC), and molecular function (GOMF) are shown. In AMPK-α1 (A) and AMPK-β1 (B), GO terms associated with the regulation of actin cytoskeletal organization were significantly enriched.

By GO analysis, both AMPK-α1- and -β1-interacting proteins were enriched in well-known process of AMPK with similar pattern, which are included in metabolic process[3,5], translation[40], RNA processing[41], gene expression[12,42], and biosynthetic process. For example, AMPK-α1- and -β1-interacting proteins were globally enriched in well-known process of AMPK regardless of affiliation, whereas AMPK-α1- and -β1-interacting proteins in Rat_only were predominantly enriched in cytoskeleton-related GO terms. The similarity in patterns between AMPK-α1 and -β1 interactors in the GO analysis might be attributed to the structural conformation of the heterotrimeric AMPK complex, which contains AMPK-α1 and -β1.

To examined the signaling pathways in our AMPK interactome, we analyzed our data using the KEGG pathway database (http://www.genome.jp/kegg/) and DAVID bioinformatics tool[32]. Sixty-three AMPK-α1- and -β1-interacting proteins in the Rat_only group fell into the following KEGG pathway categories: Ribosome, Huntington disease, Parkinson disease, Oxidative phosphorylation, Splicesome, Alzheimer disease, and Regulation of actin cytoskeleton. We noted that 7 proteins—IQGAP1, gelsolin, cofilin-1, Myh9, Myh10, Myl12b, and Myh14—regulate organization of the actin cytoskeleton, which is consistent with the GO analysis. In addition, as reported[43], vimentin was linked to actin cytoskeletal organization. Consequently, 8 novel proteins that were associated with actin cytoskeletal organization were obtained, based on the functional classification (Table 2).

Table 2. Novel interactors of AMPK associated with regulation of actin cytoskeleton

Accession Number	Gene Name	Gene Symbol	Proteins Name	Molecular Weight	Species	Observed datasets
IPI00365769	IQ motif containing GTPase-activating protein 1	**Iqgap1**	ras GTPase-activating-like protein IQGAP1	189 kDa	Rattus norvegicus	a1[a]/ b1[b]
IPI00327144	cofilin 1, non-muscle	**Cfl1**	Cofilin-1	19 kDa	Rattus norvegicus	a1[a]
IPI00363974	gelsolin	**Gsn**	Uncharacterized protein	86 kDa	Rattus norvegicus	a1[a] / b1[b]
IPI00421625	myosin regulatory light chain MRLC2	**Myl12b**	Myosin regulatory light chain 12B	20 kDa	Rattus norvegicus	a1[a] / b1[b]
IPI00391300	myosin, heavy chain 10, non-muscle	**Myh10**	Uncharacterized protein	234 kDa	Rattus norvegicus	a1[a] / b1[b]
IPI00390280	myosin, heavy chain 14	**Myh14**	Uncharacterized protein	232 kDa	Rattus norvegicus	a1[a] / b1[b]
IPI00209113	myosin, heavy chain 9, non-muscle	**Myh9**	Myosin-9	226 kDa	Rattus norvegicus	a1[a] / b1[b]
IPI00418471	Vimentin	**Vim**	Vimentin	54kDa	Rattus norvegicus	a1[a] / b1[b]

[a] Experiments using AMPK alpha-1 subunits as bait
[b] Experiments using AMPK beta-1 subunits as bait

In pancreatic beta-cells, the actin cytoskeleton has important functions in many processes, including GSIS, cell-cell adhesion, and proliferation[22,44-46]. Although it is unknown whether AMPK interacts directly with components in the actin cytoskeleton, recent studies have indicated that AMPK regulates its organization to mediate cell mobility and migration[47-49]. Hence, we focused on the interactions of proteins that are associated with actin cytoskeletal organization.

3.4. Interaction of proteins related to actin cytoskeletal organization with AMPK

To examine the interactions between proteins that regulate actin cytoskeletal organization and AMPK, we generated a protein interaction network of 138 proteins from the KEGG pathway database using STRING 9.0[33] and Cytoscape[34]. The evidence-based global STRING-generated protein network[33] showed high connectivity between actin cytoskeleton-regulating proteins (Figure 12). However, the relationship between AMPK and actin cytoskeletal organization was not well defined in the protein interaction network. Thus, we added 15 direct interactions between AMPK and 8 identified proteins to the protein interaction network (Figure 12A & Table 2).

Of the interactions that were detected by AP-MS, the binding of IQGAP1, gelsolin, and vimentin to AMPK-α1 and -β1 was confirmed by coimmunoprecipitation using 6-myc-tagged AMPK-α1 and -β1. As shown in Figure 12B, IQGAP1, gelsolin, and vimentin coimmunoprecipitated with both AMPK subunits, demonstrating that AMPK-α1 and -β1 bind to the actin cytoskeleton.

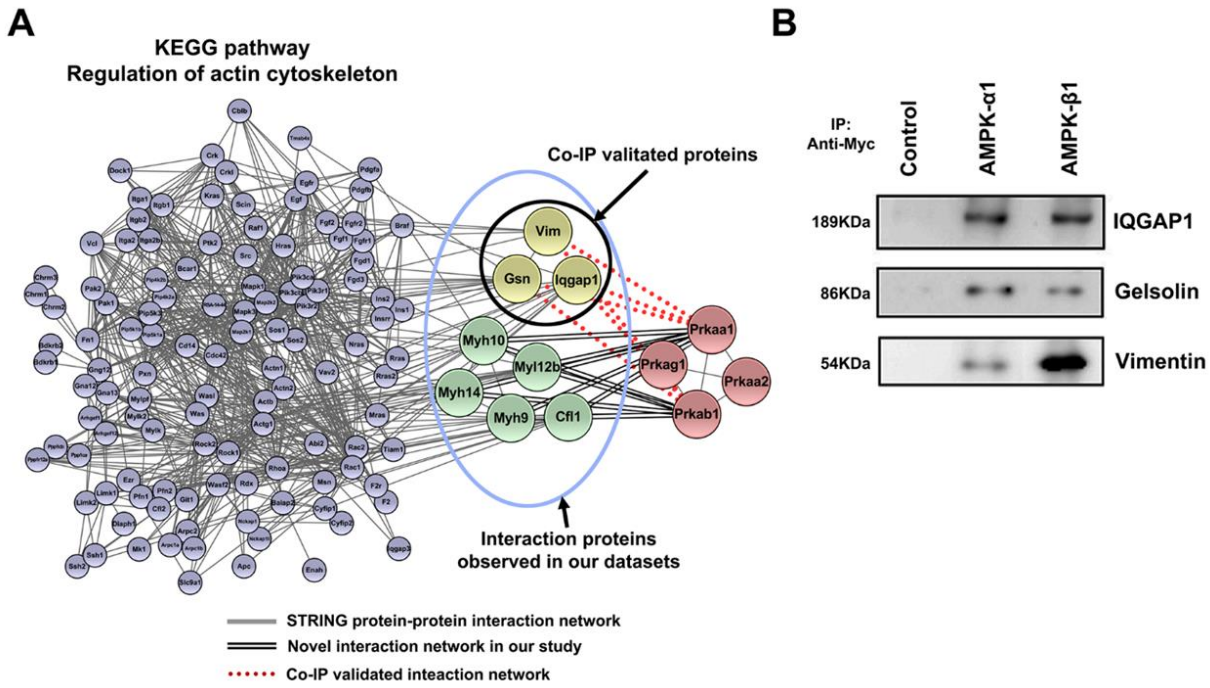

Figure 12. Interaction network for proteins associated with AMPK complex in regulation of actin cytoskeleton

(A) Network analysis of AMPK interactome, showing that the AMPK complex interacts directly with multiple proteins associated with the regulation of the actin cytoskeleton. Proteins and protein-protein interactions associated with regulation of the actin cytoskeleton were extracted from the KEGG pathway and STRING 9.0 (http://string-db.org/) databases. All input proteins associated with actin regulation are depicted as small blue spheres. Interacting proteins in our dataset are depicted as green spheres, and interacting proteins validated by Co-IP are shown as yellow spheres. AMPK subunit proteins are shown as red spheres. Protein-protein interactions extracted from the STRING database are shown as grey lines. Interactions identified in this study are shown as black double lines. Co-IP-validated interactions are shown as red dotted lines. (B) Validation of protein-protein interactions. IQGAP1, gelsolin, and vimentin were validated by Co-IP and western blot. Myc-tagged bait proteins (AMPK-α1 and AMPK-β1) were expressed in HEK293T cells, mixed with INS-1 cell lysates, and immunoprecipitated using anti-Myc. Immunoprecipitated proteins were analyzed by western blot using antibodies against IQGAP1, gelsolin, and vimentin.

IV. RESULTS (II)

4. Direct immunoprecipitation in INS-1 pancreatic beta-cell

4.1. Overall scheme for profiling of AMPK-α1 and -β1 interactomes

Further we have performed a comprehensive AP-MS analysis, combining pulldown assay based on tagged recombinant baits and direct immunoprecipitation (direct IP) for endogenous target proteins, to increase the coverage. HEK293T control experiments for pulldown approach and direct IP was performed in INS-1 cells to minimize false positives in the pulldown experiments. In the control experiments, the species affiliation analysis distinguishes the origin of the proteins (rat or human) that have been pulled down from INS-1 cell extracts with myc-AMPK-α1 and AMPK-β1. All experiments were repeated (4 biological replicates per bait), and agarose datasets in the original experiment that had low reproducibility were removed.

The AP-MS data were processed using the SAINT algorithm instead of fold-changes to increase confidence of the interactome data. Six proteins that are related to actin remodeling, including 4 novel interactors (Iqgap1, Myh9, Rhoa, and Rac1), were validated by co-IP in INS-1, pancreatic beta cells.

We performed several new experiments, refined the statistical analysis, and conducted more experimental validation to improve our data compared with the original experiment.

To identify the interactomes of AMPK-α1 and AMPK-β1 in pancreatic beta-cells, we performed a comprehensive AP-MS analysis, combining pulldown experiments using tagged recombinant baits and direct immunoprecipitation (direct IP) of endogenous target proteins (Figure 13).

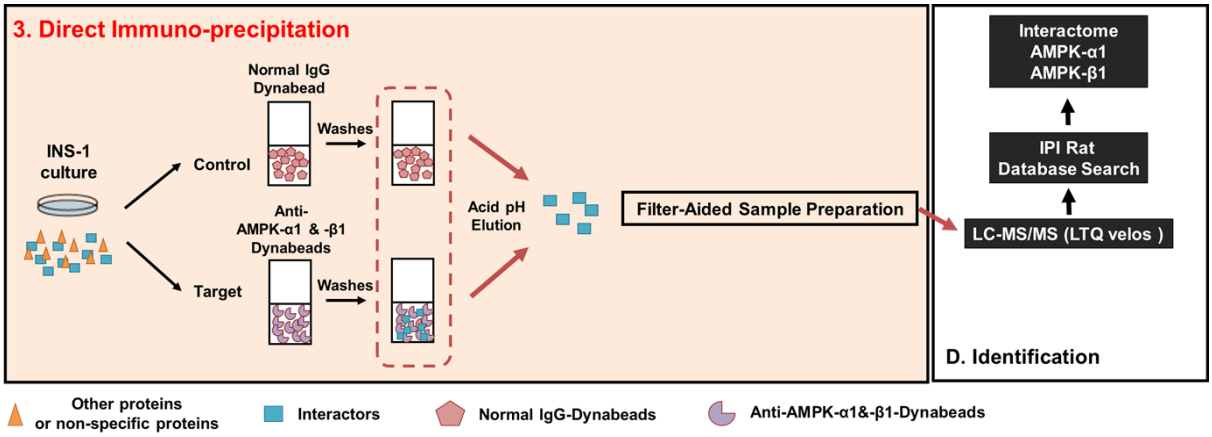

Figure 13. Experimental scheme to examine interactomes of AMPK subunits

To compare protein interactions, we performed pulldown and direct immunoprecipitation (IP).

In the direct IP, endogenous AMPK subunits were immunoprecipitated in INS-1 cells. For elimination of contam lists in affinity puripication, interacting proteins between the control and target AMPK groups were analyzed using Scaffold 4.

Initially, we planned to overexpress 6-myc epitope-tagged AMPK-α1 and AMPK-β1 by transfection in INS-1 cells. However, we could not obtain a sufficient amount of myc-tagged proteins to perform AP-MS, due to the low transfection efficiency of INS-1 cells (Figure 3A). Alternatively, we overexpressed N-terminally 6-myc-tagged rat AMPK-α1 and AMPK-β1 in HEK293T cells and immobilized them to Dynabeads (Figure 4A, Dynabeads set). Briefly, to express the recombinant proteins, full-length rat AMPK-α1 and -β1 cDNA was subcloned into modified pcDNA3.1 and transfected into HEK293T cells by PEI method[23,24].

For the pulldown approach (Figure 4A, Dynabeads set), we used magnetic beads (Dynabeads) as the IP material. Recombinant AMPK subunits from 1 mg of transfected HEK293T cells were immobilized using anti-myc-conjugated Dynabeads. To prevent any bias from immobilization of the antibody, anti-myc-conjugated Dynabeads that were incubated with mock-transfected HEK293T lysates were used as bait in the negative control experiment (Figure 4A, Dynabeads set). To remove nonspecific lysate products, INS-1 lysates were precleared with the same material as in the IP (Figure 4B)[36]. Subsequently, the immobilized 6-myc-tagged AMPK-α1 and -β1 were used as bait in pulldown assays with 1 mg of INS-1 lysate (Figure 4C). Eluted samples from the bait production (Figure 4A, Dynabeads set) were analyzed by LC-MS/MS to confirm the coelution of false-positive interactors and to examine homologous interactions in HEK293T cells. (Figure 4A, HEK293T control experiments).

The proteins that coprecipitated with the myc-tagged baits were separated on a 1-DE 10% bis-tris SDS-PAGE gel and subjected to in-gel trypsin digestion. Finally, the peptide mixtures were desalted using C_{18}-Stagetips[25] and analyzed on an LTQ Velos linear ion trap LC-MS/MS system (Figure 4D). Two biological replicates and 3 technical replicates were analyzed.

Further, to increase the coverage and enhance the reliability of the AMPK interactome, direct IP was performed without overexpression of the target baits (Figure 13). Briefly, native protein complexes were isolated directly using antibodies against AMPK-α1 and AMPK-β1 from 10 mg of INS-1 cell lysate. Anti-IgG served as the negative control. The proteins that coprecipitated with the endogenous baits were eluted with acid buffer and subjected to filter-aided sample preparation (FASP)[26,27]. Finally, peptide desalting and MS analysis were performed as described above (Figure 13).

Consequently, we generated 4 datasets of the AMPK interactome (AMPK-α1 pulldown, AMPK-α1 direct IP, AMPK-β1 pulldown, and AMPK-β1 direct IP); all experiments were performed with biological duplicates and technical triplicates.

Expression, immobilization, and pulldown were verified by western blot (Figure 3). Overexpression of myc-tagged AMPK-α1 and -β1 in HEK293T cells was confirmed by western blot with anti-myc, whereas we could not detect any myc-tagged proteins in INS-1 cells (Figure 3A). Western blot with AMPK-α1 and -β1 antibodies was also performed to verify the immobilization and coelution of AMPK-α1 and -β1 in the elution fractions of each IP step. AMPK-α1 and -β1 were detected in the elution fractions of the target baits but not the mock control lane in the pulldown (Figure 3C), indicating that our approach reliably identified interactors of the targets of interest.

Finally, aliquots of the pulldown and immunoprecipitation fractions were loaded onto an SDS-PAGE gel and stained with silver nitrate. Bands that appeared to correspond to AMPK-α1 and -β1 and their interacting partners were observed in the target bait IP (Figures 14A & 14B).

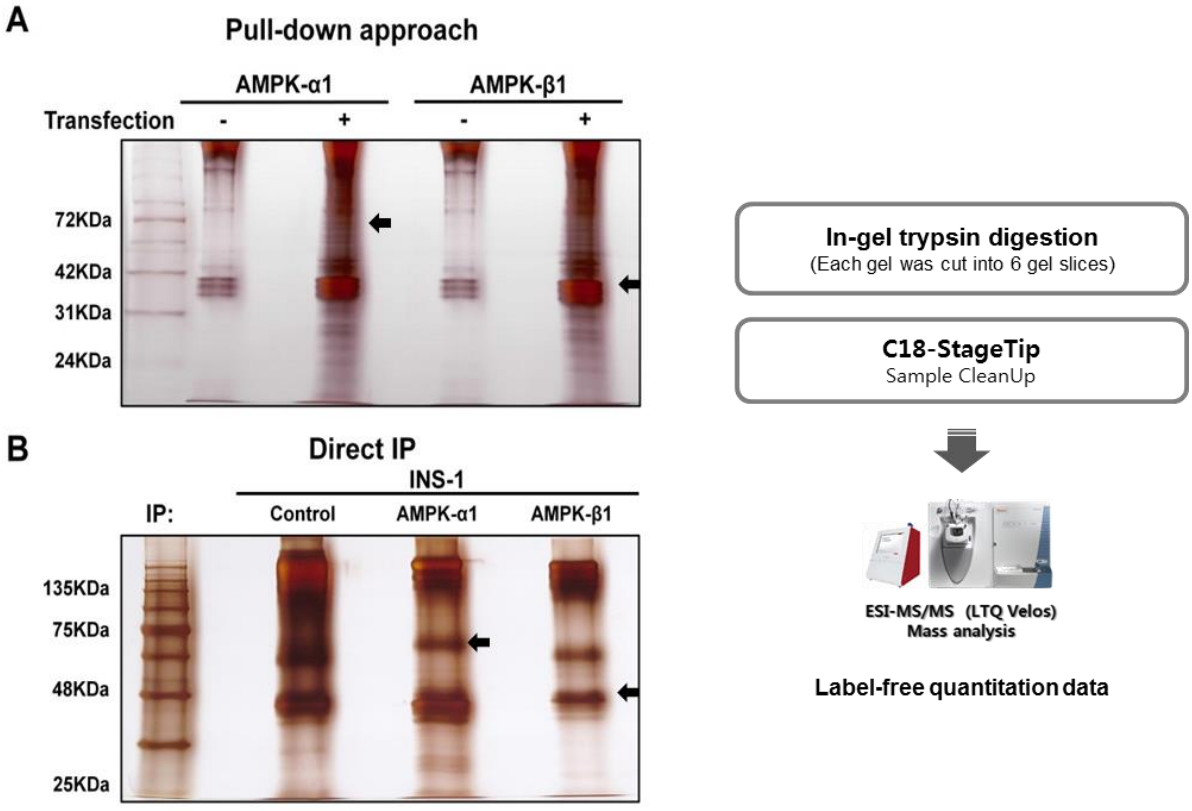

Figure 14. Representative 1D-gel image of affinity purification

In the pulldown approach (A) and direct IP (B), the immunoprecipitates were eluted with citrate buffer and separated on a 1D 10% Bis-Tris SDS-PAGE gel. Each gel was cut into 6 gel slices, each of which was subjected to in-gel trypsin digestion.

4.2. Identification of novel AMPK-α1- and –β1- interacting proteins

For the pulldown approach, recombinant rat AMPK subunits were overexpressed as baits in HEK293T cells, suggesting that some of the identified interactors originated from human cells. Thus, the proteins that interact with AMPK subunits in INS-1 cells must be classified with regard to species. To separate the interacting proteins that were derived solely from HEK293T cells, MS/MS spectra were searched on the Sorcerer-SEQUEST platform[28] using a target-decoy strategy against a concatenated database that contained the human IPI database (version 3.87, 91,464 entries), rat IPI database (version 3.87, 39,925 entries), and their reverse-complements. Conversely, for the direct IP approach, MS/MS spectra were searched only in the Sorcerer-SEQUEST platform[28] using a target-decoy strategy against a concatenated database of the rat IPI database. All search results were validated and filtered using Scaffold 4 to establish AP-MS datasets at an FDR < 1.0% (Figure 15A).

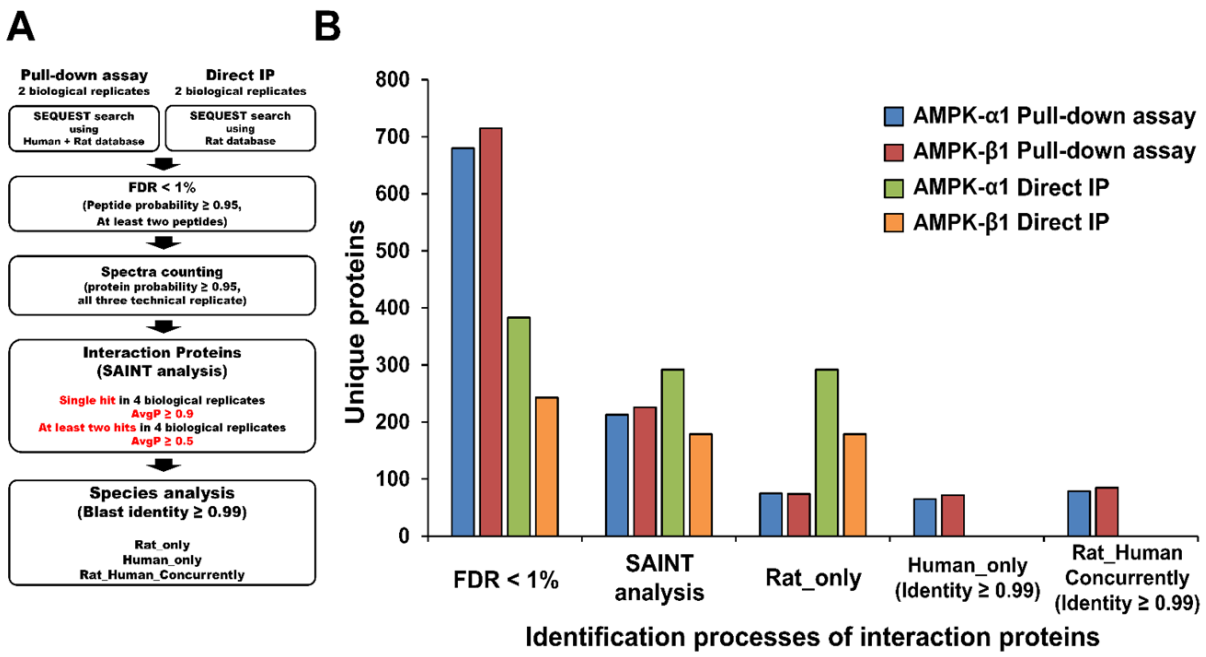

Figure 15. Strategy of SAINT analysis for interactome

To remove nonspecific interactors, we used stringent filtering criteria and the SAINT algorithm. (A) Flowchart of data processing for AMPK interactome. MS datasets from the pulldown assay and direct IP were filtered sequentially with the filtering criteria. Further, SAINT, species affiliation, and BLAST analysis were performed consecutively to differentiate high-confidence interactors and nonspecific contaminants. (B) Identification of proteins that interact with AMPK-α1 and -b1 subunits. The number of identified proteins is shown for each stage of the data processing. AMPK-α1 pulldown assay, AMPK-b1 pulldown assay, AMPK-α1 direct IP, and AMPK-b1 direct IP are labeled in blue, red, green, and orange, respectively.

Raw data on 36 LC-MS/MS spectra were collected, resulting in 20,421 unique spectra; 18,377 unique peptides, corresponding to 1233 unique proteins, were identified at an FDR of 1%. In experiments in which AMPK-α1 was used as bait, an average of 286 and 443 unique proteins were identified in the 2 biological replicates of the pulldown and direct IP approaches, respectively. With AMPK-β1 as bait, an average of 179 and 447 unique proteins were identified in the 2 biological replicates of the pulldown and direct IP approaches, respectively (Table 3).

Table 3. Summary of mass spectrometry analysis

Exp.	IP Baits	Identifications									Filtered data set by SAINT [Identity≥0.99]			
		Proteins			Unique Peptides			Unique Spectra			Unique proteins			
		Control baits	Target baits	Total Number of Protein	Control baits	Target baits	Total Number of Peptide	Control baits	Target baits	Total Number of Spectra	Rat Only	Rat & Human Concurrently	Human Only	Total Number of Protein
Direct IP_ Bio1	AMPK-α1	278	349	352	1092	2194	2382	1284	2602	2877	273	-	-	273[a] (271)[b]
	AMPK-β1	201	216	223	1035	1143	1507	1227	1322	1833	163	-	-	163 (162)
Direct IP_ Bio2	AMPK-α1	164	218	220	560	1322	1400	643	1527	1640	175	-	-	175 (173)
	AMPK-β1	119	132	135	536	749	876	619	898	1057	104	-	-	104 (102)
Pull down_ Bio1	AMPK-α1	283	596	599	844	3377	3626	1050	4249	4573	52	64	58	174 (173)
	AMPK-β1	291	641	645	842	3944	4206	1048	5026	5377	60	74	62	196 (193)
Pull down_ Bio2	AMPK-α1	140	284	287	619	2135	2302	785	2846	3064	47	31	37	115 (112)
	AMPK-β1	122	246	248	571	1941	2078	704	2417	2610	36	31	33	100 (99)

a. The number of the identified proteins

b. The number of the identified gene symbols

Bait recovery of the pulldown approach yielded an average of 294 and 299 spectral counts with 33% and 57% coverage for tagged AMPK-α1 and -β1, respectively. In addition, bait recovery of the direct IP approach generated an average of 42 and 20 spectral counts with 17% and 11% coverage for tagged AMPK-α1 and -β1, respectively. Because AMPK-α1 and -β1 form a complex in cells, we examined whether AMPK subunits were detected in our datasets to determine the reliability of our proteomic approaches. As shown in Figure 16, nearly all AMPK subunits that were expressed in pancreatic beta-cells, such as AMPK-α1, AMPK-α2, AMPK-β1, and AMPK-γ1, were identified with the target baits, whereas the control baits did not contain the spectral counts of AMPK subunits. These results indicate that our AP-MS approaches are reliable.

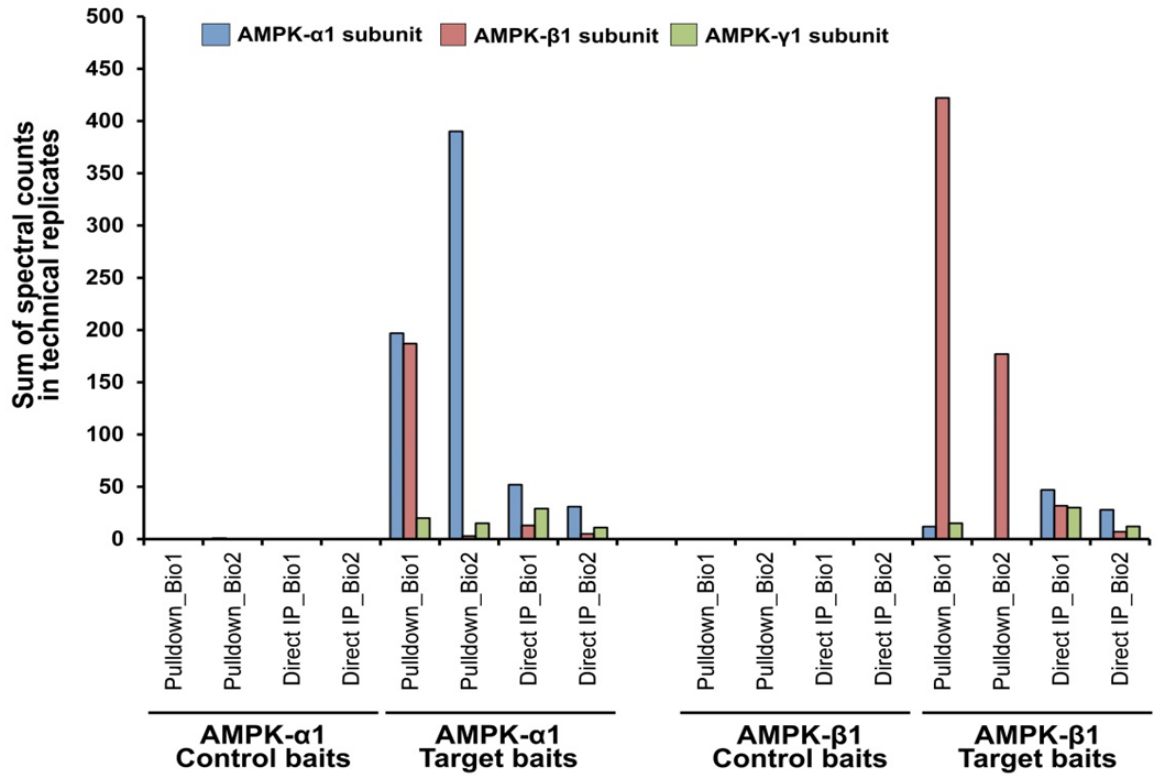

Figure 16. Spectral count distribution of AMPK subunits.

Spectral counts of AMPK-α1 (blue), AMPK-β1 (red), and AMPK-γ1(green) were taken in 3 replicate experiments, which are displayed in bars. Spectral counts were expressed as the sum of the spectral counts of 3 technical replicates.

To remove nonspecific interactors, we performed SAINT analysis[29], as shown in Figure 15A. First, in each experiment, unweighted spectral counts of proteins that were identified in the samples that corresponded to the control and baits were exported from Scaffold 4. Then, to include only high-confidence proteins, proteins had to have been identified in all 3 technical replicates with a protein probability score ≥ 0.95 to be input into the SAINT analysis. In 4 individual experiments per target bait, identifications were accepted for proteins that appeared in at least 2 experiments with an average individual probability for SAINT analysis (AvgP SAINT) ≥ 0.50. In addition, single-protein hits were considered positive at AvgP SAINT ≥ 0.90.

Finally, for the pulldown approach, the amino acid sequences of the filtered proteins were examined with regard to species using the protein grouping algorithm in Scaffold 4 to sort INS-1-specific interactors. In Scaffold 4, proteins that are identified with the same sequence of a peptide (ie, the sharing peptide) are represented as protein groups. Because we used a concatenated human and rat database in the pulldown approach, we could verify whether the identified proteins were human or rat. For example, if a protein group comprises only rat proteins, it clearly matches rat proteins—not its human orthologous counterpart. However, if a protein group contains a mixture of human and rat proteins, we can conclude that it was derived from HEK293T or INS-1 cells.

Thus, the proteins that were identified in the pulldown approach were classified into 3 groups: Rat_only, Rat_Human_Concurrently, and Human_only. To avoid missed interactions and recover homologous interactions in the pulldown approach, only proteins in the Rat_Human_Concurrently and Human_only groups that had at least 99% sequence identity between the rat and human homologs were included in the final list by BLAST analysis (Figure 15B). In total, 325 AMPK-α1 and 243 AMPK-β1 interactors were identified in this study and classified as the “INS-1 specific group”. In addition, 97 AMPK-α1- and 92 AMPK-β1-binding partners in the HEK293T control experiments (the human species group, Fig 7A, HEK293T control experiments) are shown in. For further analysis, the HEK293T

control experiments were processed under the same conditions as with the INS-1-specific group.

4.3. Functional classification of AMPK-specific interactors

To determine the functions of proteins that interact with AMPK subunits in INS-1 cells, the AMPK-α1 and -β1 binding partners were grouped by Gene Ontology (GO) term using the DAVID bioinformatics resource tool into biological process, cellular compartment, and molecular function[32]. To identify the GO categories that were overrepresented in proteins in INS-1 cells, the INS-1-specific groups and human species group were subjected individually to GO analysis (Figure 17).

By GO analysis, AMPK-α1- and -β1-interacting proteins were enriched globally in AMPK-mediated processes with similar patterns, regardless of species affiliation (Figures 17A and 17B). For example, the commonly enriched categories in the 2 groups of the datasets were linked to major pathways that are associated with AMPK, such as metabolism[3,5], translation[40], and biosynthesis. Also, most proteins were distributed broadly throughout the cytosol, mitochondria, nucleolus, and ribosome. AMPK-α1- and -β1-interacting proteins that mediate the organization and regulation of the actin cytoskeleton were significantly enriched in the INS-1-specific versus human species group (Figures 17A and 17B). In addition, many proteins in the INS-1-specific group were involved in transport, the cell cycle, and cytoskeletal protein binding. The similarity in patterns between AMPK-α1 and -β1 interactors in the GO analysis might be attributed to the structural conformation of the heterotrimeric AMPK complex, which contains AMPK-α1 and -β1.

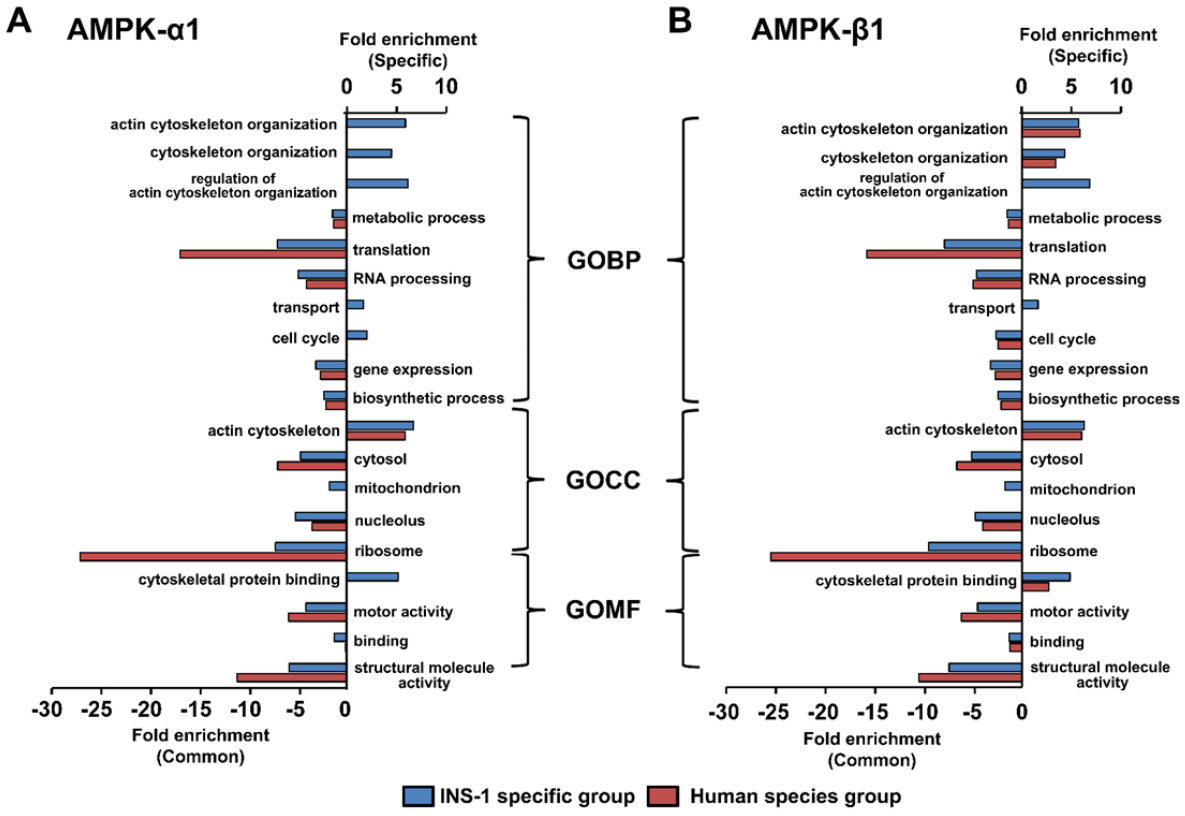

Figure 17. Functional GO annotation of AMPK-α1 and AMPK-β1 interactome

All identified proteins—325 AMPK-α1- and 243 AMPK-β1-interacting proteins—were grouped, based on GO terms. GO terms enriched from proteins identified in INS-1 specific group were classified as specific, whereas those from proteins in the INS-1-specific and Human species groups were classified as common. Fold-enrichment for a particular GO term describes the ratio between the numbers of genes belonging to a specific GO term and the total number of genes in the genome with at least 1 GO annotation. Enriched GO terms for biological process (GOBP), cellular component (GOCC), and molecular function (GOMF) are shown. In AMPK-α1 (A) and AMPK-β1 (B), GO terms associated with the regulation of actin cytoskeletal organization were significantly enriched.

To examine the signaling pathways in our AMPK interactome, we analyzed our data using the KEGG pathway database (http://www.genome.jp/kegg/) and DAVID bioinformatics tool[32]. A total of 381 AMPK-α1- and -β1-interacting proteins in the INS-1-specific group fell into the following KEGG pathway categories: Ribosome, Spliceosome, Huntington disease, Parkinson disease, Adherens junction, and Regulation of actin cytoskeleton. Notably, KEGG pathway analysis of the human species groups demonstrated that only proteins in the INS-1-specific groups were significantly enriched with regard to regulation of the actin cytoskeleton.

Fifteen proteins regulated organization of the actin cytoskeleton, which is consistent with the GO analysis. In addition, based on a literature search[43], Myl12b was linked to actin cytoskeletal organization. Consequently, 16 proteins that were associated with actin cytoskeletal organization were obtained, based on the functional classification (Table 4).

In pancreatic beta-cells, the actin cytoskeleton has significant functions in many processes, including GSIS, cell-cell adhesion, and proliferation[22,44,45]. Although whether AMPK interacts directly with components in the actin cytoskeleton is unknown, recent studies have indicated that AMPK regulates its organization to mediate cell mobility and migration[47-49]. Based on the novelty of these results, we focused on the interactions of proteins that are associated with actin cytoskeletal organization.

Table 4. Novel interactors of AMPK associated with regulation of actin cytoskeleton

Gene Symbol	Protein Name	Molecular Weight	Species	baits	Novel
Iqgap1	IQ motif containing GTPase activating protein 1	189 kDa	Rattus norvegicus	α1/β1	O
Arpc4	actin related protein 2/3 complex, subunit 4	20 kDa	Rattus norvegicus	α1	O
Actg1	actin, gamma 1	42 kDa	Rattus norvegicus	α1/β1	O
Actn4	actinin alpha 4	105 kDa	Rattus norvegicus	α1/β1	O
Actn1	actinin alpha 1	103 kDa	Rattus norvegicus	α1/β1	O
Cfl1	cofilin 1, non-muscle	19 kDa	Rattus norvegicus	α1	O
Cfl2	cofilin 2, muscle	19 kDa	Rattus norvegicus	β1	O
Gsn	Gelsolin	86 kDa	Rattus norvegicus	α1/β1	X
Myh10	myosin, heavy chain 10, non-muscle	234 kDa	Rattus norvegicus	α1/β1	X
Myh14	myosin, heavy chain 14	232 kDa	Rattus norvegicus	β1	X
Myh9	myosin, heavy chain 9, non-muscle	226 kDa	Rattus norvegicus	α1/β1	O
Ppp1ca	protein phosphatase 1, catalytic subunit, alpha isoform	38 kDa	Rattus norvegicus	α1/β1	O
Ppp1cb	protein phosphatase 1, catalytic subunit, beta isoform	37 kDa	Rattus norvegicus	β1	O
Rhoa	ras homolog gene family, member A	22 kDa	Rattus norvegicus	α1	O
Rac1	ras-related C3 botulinum toxin substrate 1	21 kDa	Rattus norvegicus	α1/β1	O
Myl12b	myosin regulatory light chain MRLC2	20 kDa	Rattus norvegicus	α1/β1	O
Vim	Vimentin	54 kDa	Homo sapiens	control	X

4.4. Interaction of proteins related to actin cytoskeletal organization with AMPK

To examine the interactions between proteins that regulate actin cytoskeletal organization and AMPK, we generated a protein interaction network of 140 proteins from the KEGG pathway database using STRING 9.1[33] and Cytoscape[34]. The evidence-based global STRING-generated protein network[33] showed high connectivity between actin cytoskeleton-regulating proteins (Figure 18A). However, the relationship between AMPK and actin cytoskeletal organization was not well defined in the protein interaction network. Thus, we added 28 direct interactions between 17 actin cytoskeleton-related proteins and AMPK-α1/-β1 to the protein interaction network (Figure 18A & Table 4).

Of the interactions that were detected by AP-MS, the binding of Iqgap1, Gsn, and Vim to AMPK-α1 and -β1 was confirmed by coimmunoprecipitation using 6-myc-tagged AMPK-α1 and -β1. As shown in Figure 18B, IQGAP1 and gelsolin (Gsn) coimmunoprecipitated with both AMPK subunits. Vimentin was used as the positive control, based on the robust interaction between vimentin and AMPK.

The interaction with Myh9, IQGAP1, Rhoa, and Rac1 was validated by direct coimmunoprecipitation in INS-1 cells (Figure 18C). The interaction between AMPK-α1 and -β1 was tested as the positive control. In total, we validated the interactions of 6 proteins (Gsn, Iqgap1, Vim, Myh9, Rhoa, and Rac1) that were linked to regulation of the actin cytoskeleton, demonstrating that AMPK-α1 and -β1 bind to the actin cytoskeleton and interact physically with regulators of the actin cytoskeleton organization.

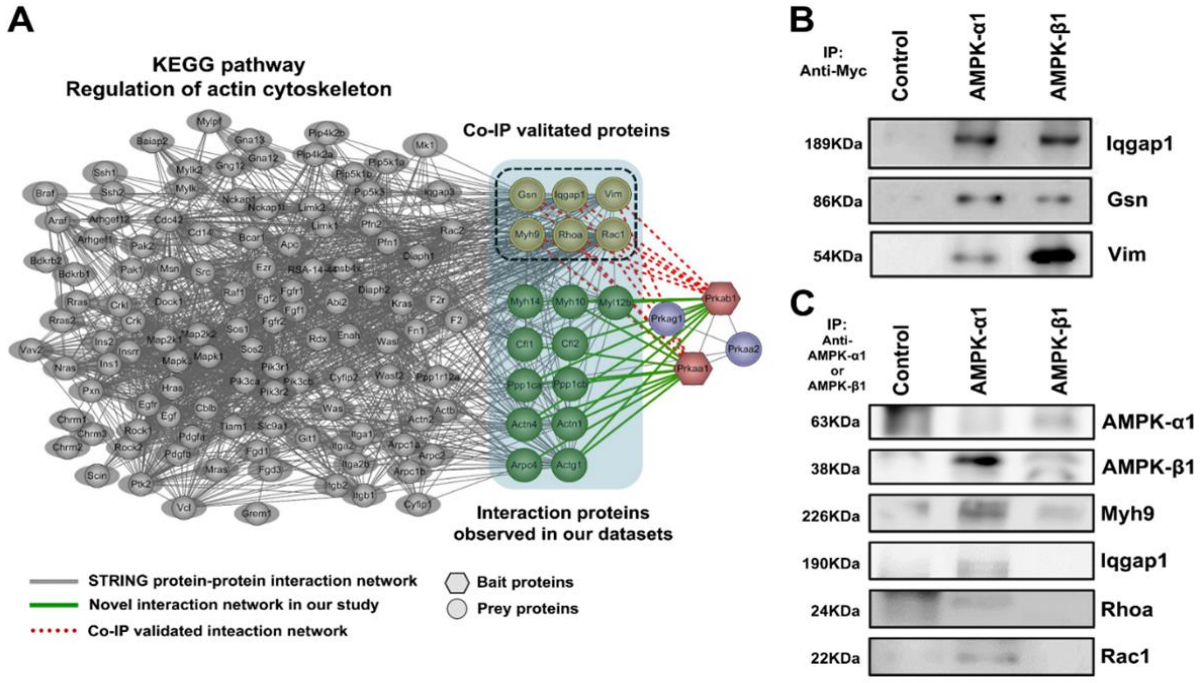

Figure 18. Interaction network for proteins associated with AMPK complex in regulation of actin cytoskeleton

(A) Network analysis of AMPK interactome, showing that the AMPK complex interacts directly with multiple proteins associated with the regulation of the actin cytoskeleton. Proteins and protein-protein interactions associated with regulation of the actin cytoskeleton were extracted from the KEGG pathway and STRING 9.1 databases. All input proteins associated with actin regulation are depicted as small gray spheres. Interacting proteins in our dataset are depicted as green spheres, and interacting proteins validated by Co-IP are shown as yellow spheres. Bait proteins are shown as red hexagons. Protein-protein interactions extracted from the STRING database are shown as grey lines. Interactions identified in this study are shown as green lines. Co-IP-validated interactions are shown as red dotted lines. (B) Validation of protein-protein interactions by pulldown approach. A novel interacting protein (Iqgap1) was validated by co-IP. Well-known proteins (Gsn and Vim) were also validated. Vim was used as a positive control to confirm homologous interactions. (C) Validation of protein-protein interactions using direct IP. AMPK-α1, AMPK-β1, Myh9, Iqgap1, Rhoa, and Rac1 were validated by co-IP. The co-IP results for novel interactors (Myh9, Iqgap1, Rhoa, and Rac1) that were associated with regulation of the actin cytoskeleton corresponded well with the AP-MS results.

V. DISCUSSION

The aim of this study was to identify AMPK-interacting proteins in pancreatic beta-cells. For the AP-MS analysis, we first examined the expression of tagged baits in HEK293T cells, a cell type that has high transfection rates, because INS-1 beta-cells have low transfection efficiency of DNA vectors. Although we tried to exclude binding partners that arose solely from the HEK293T cells through a negative control experiment and species affiliation analysis with a combination database (human and rat) search, it is possible that false-positive interactors and overlooked interactions existed in our pulldown approach.

Because we combined the IPI Human and Rat databases, the IPI accession numbers of the identified proteins were converted to gene names (symbols) and subjected to comparison analysis. Of the 784 proteins in our interactome, 658 gene symbols were obtained. The Venn diagrams in Figures 7D and 7E show the overlap in unique proteins between 2 approaches (agarose beads and Dynabeads) for AMPK-α1 and -β1, respectively. Comparisons between groups (Rat_only, Rat_Human_concurrently, and Human_only) in the AMPK-α1 set indicated that the overlap between agarose and Dynabeads ranged from 5.6% to 16.2% (Figures 10A–10C). Also, for AMPK-β1, the overlap between agarose and Dynabeads ranged from 8% to 20.5% (Figures 10D – 10F). These results demonstrate that our approaches with various IP materials provide complementary coverage and that their combination effects comprehensive coverage of the AMPK-α1 and -β1 interactome.

However, the overlap between datasets was relatively low, possibly due to differences in sample preparation methods for the agarose and Dynabead sets. Our approaches using agarose beads and Dynabeads had biological and technical variation, because the starting material was generated under the same conditions. In addition, the use of low-resolution mass spectrometry can result in analytical variation[50]. Although the low overlap between experiments demonstrates that our approaches with

disparate IP materials have a slight bias, they identified distinct segments of the AMPK interactome and enhanced coverage of the AMPK interactome. Notably, between the AMPK-α1 and AMPK-β1 datasets that were merged from different methods, there was 56% overlap (371 per 658 proteins), which is better than that of each method (Figure 7F).

To verify the reliability of the species affiliation analysis in the pulldown approach, we performed several preliminary control experiments. In generating the tagged AMPK baits (Figure 4A), the proteins that were considered to have originated from HEK293T cells were analyzed by LC-MS/MS without incubation with INS-1 cell extracts (Fig 4A, HEK293T control experiments), whereas the baits was incubated with INS-1 cell extracts in the pulldown assay (Figures 4B & 4C). These experiments indicated that that species affiliation analysis distinguished the origins of proteins in the pull-down of INS-1 cell extracts with myc-AMPK-α1 and -β1 (Figure 19A).

Further, BLAST analysis was performed to prevent missed interactions and increase the sensitivity in the pulldown assay. Only proteins with at least 99% sequence identity between the human and rat orthologs in the Rat_Human_Concurrently and Human_only groups were included in the final list. To ensure the specificity of the BLAST analysis, vimentin (98% sequence identity between human and rat), an interactor of AMPK-α and –β[21,52], was used as the positive control. Despite its sequence identity (98%), we confirmed a homologous interaction between vimentin and AMPK subunits (Figure 18B), suggesting that the BLAST analysis could rescue a homologous interaction in the pulldown approach.

As shown in Figure 19B, our BLAST analysis recovered approximately 50% of proteins that were identified as Human_only and Rat_human_concurrently after the filtration per the 99% sequence identity criterion. Moreover, the similar distribution of sequence identities in the HEK293T control experiments demonstrates that the BLAST analysis was not biased against the pulldown assay (Figure 19B).

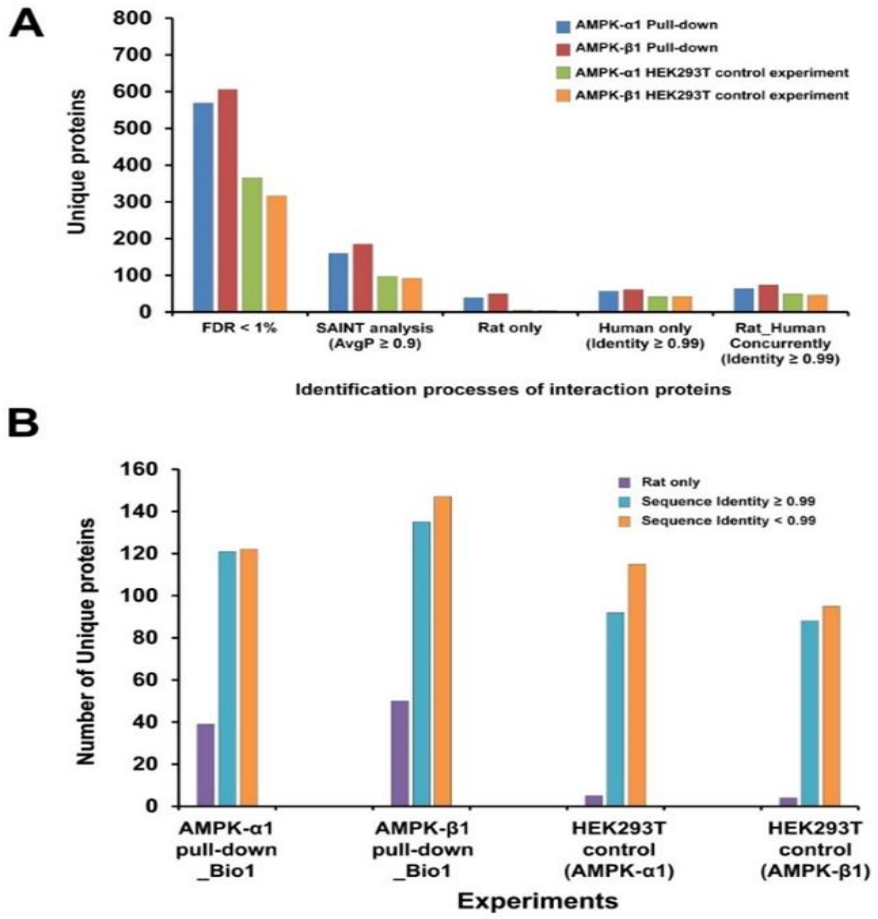

Figure 19. Comparison between pull down approach and HEK293T control experiments.

(A) Identification of proteins that interact with AMPK-α1 and -b1 subunits in the pulldown approach and HEK293T control experiments. The number of identified proteins is displayed for each stage. AMPK-α1 pulldown, AMPK-b1 pulldown, AMPK-α1 HEK293T control experiment, and AMPK-b1 HEK293T control experiment are labeled blue, red, green, and orange, respectively. (B) Sequence identity analysis using BLAST between biological replicate 1 of AMPK-α1/-b1 and HEK293T control experiments (AMPK-α1/-b1). Proteins identified as Human_only and Rat_Human_Concurrently, except for Rat_only, were subjected to sequence identity analysis. The number of identified proteins is shown. Proteins identified as Rat_only are labeled purple. Proteins with sequence identity of at least 0.99 and below 0.99 are labeled blue and orange, respectively.

To overcome the limitations of the pulldown assay and increase coverage of the AMPK interactome with high confidence, direct IP was performed using antibodies against AMPK-α1 and -β1 in INS-1 cells without overexpression of baits. In addition, the pulldown and direct IP experiments were repeated independently with each bait and processed using the SAINT algorithm[29]. The SAINT statistical platform allowed us to assign confidence scores to interacting proteins from our AP-MS experiments. SAINT uses spectral counts of identified proteins to derive a probability score of a true interaction and discerns true interaction partners from background noise[29].

Thus, we used a stringent AP-MS strategy that was complemented by bioinformatics, SAINT analysis, and affinity purification—combining pulldown assay and direct immunoprecipitation—to draft the AMPK-α1 and -β1 interactome in INS-1 pancreatic beta-cells. Because we combined the Human and Rat IPI databases in the pulldown assay, the IPI accession numbers of the identified proteins were converted to gene names (symbols) and subjected to comparison analysis.

The Venn diagrams in Figures 20A show the overlap in unique proteins between the pulldown assay and direct IP for AMPK-α1 and -β1. These results demonstrate that our approaches provide complementary coverage and that their combination effects comprehensive coverage of the AMPK-α1 and -β1 interactomes. Although the overlap between datasets was low due to biological and technical variations between the approaches and the use of low-resolution mass spectrometry[50], 201 (62%) and 116 (48%) proteins were identified in at least 2 of 4 biological replicates for AMPK-α1 and -β1, respectively. Notably, between the AMPK-α1 and AMPK-β1 datasets that were merged from the approaches, there was 58% to 77% overlap (187 of 325 and 243 proteins in AMPK-α1 and AMPK-β1 each, respectively), which is better compared with the individual methods (Figure 20B). Although the overlap between experiments was not high, the approaches enhanced coverage and identified distinct segments of the AMPK interactome.

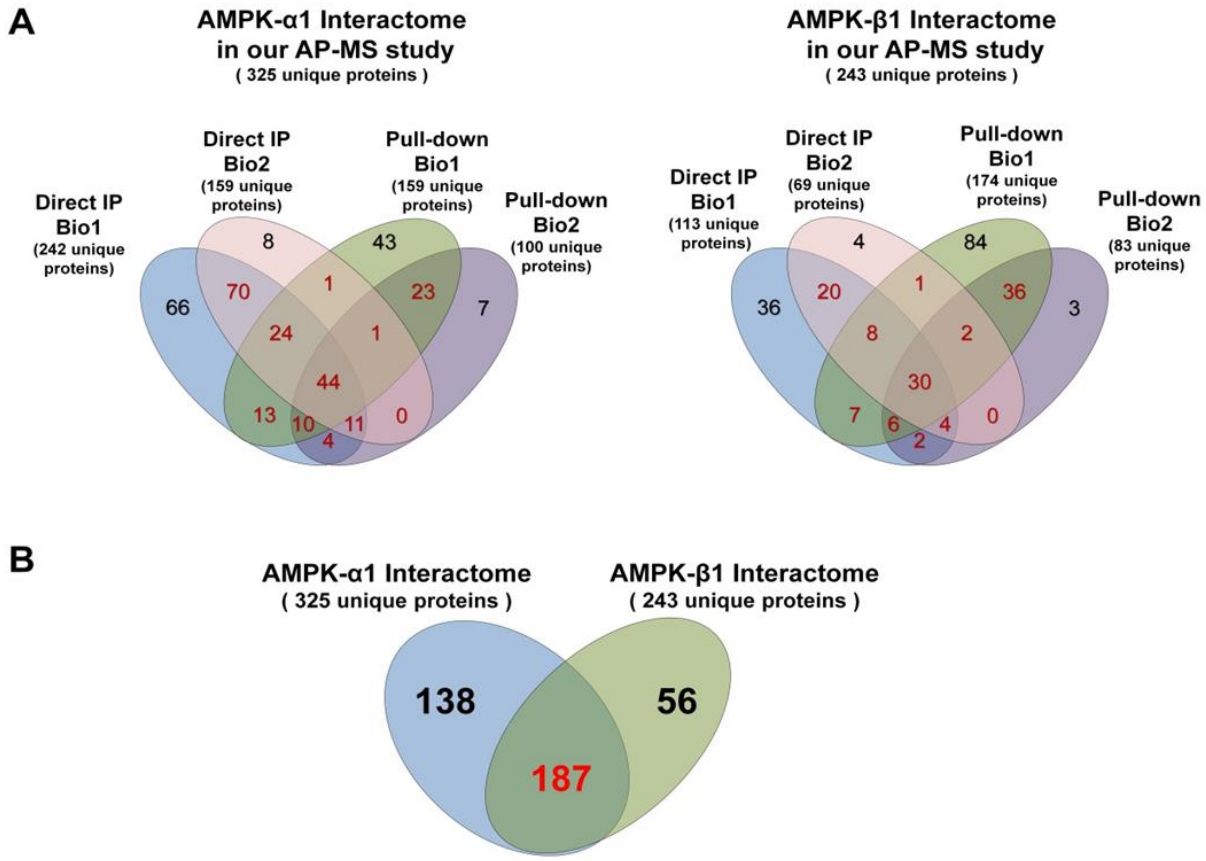

Figure 20. Comparison between numbers of interaction proteins identified by stringent criteria and SAINT analysis

(A) Venn diagrams of the overlap in interaction proteins between 4 biological replicates for AMPK-α1 and AMPK-β1. (B) Venn diagrams of the overlap between the AMPK-α1 and AMPK-β1 interactomes.

5.1. Comparison with other proteomics studies

We compared our AMPK-α1 and -β1 interactome with existing data. Although several partners of AMPK-α1 and -β1 have been reported[21,52,71], no global interactome analysis has focused on AMPK subunits. In particular, none of the well-characterized partners of these subunits have been identified in pancreatic beta-cells, based on mass spectrometry.

Large-scale proteomic data on AMPK interactors have been reported by Behrends et al.[21], Pilot-Storch et al.[71], and Varjosalo et al.[52] in human cell lines. The 614 proteins in these reports were compared directly with our AMPK-α1 and -β1 interactors, based on gene name (symbol) (Figure 21A). Of the 381 proteins in our list, there were 145 proteins with the same gene name in the 3 datasets. In addition, we compared our interactome with a public database[72]. A total of 253 interactions for AMPK-α1 and -β1 were obtained from the Protein Interaction Network Analysis (PINA) 2.0 database[72], 41 of which were common between our interactome and the database (Figure 21B). Further, our data were compared with the results of the protein-protein interaction prediction by the PrePPI server[73], which included 736 and 675 interactions of AMPK -α1 and -β1 in human cells, respectively, 63 of which were found in our data (Figure 21C). Collectively, 185 (48%) proteins in our interaction data were identified in other studies, and 196 (52%) proteins were postulated to be novel (Figure 21D). Considering all comparison analyses, our dataset contains a substantial amount of new information on AMPK-specific interaction.

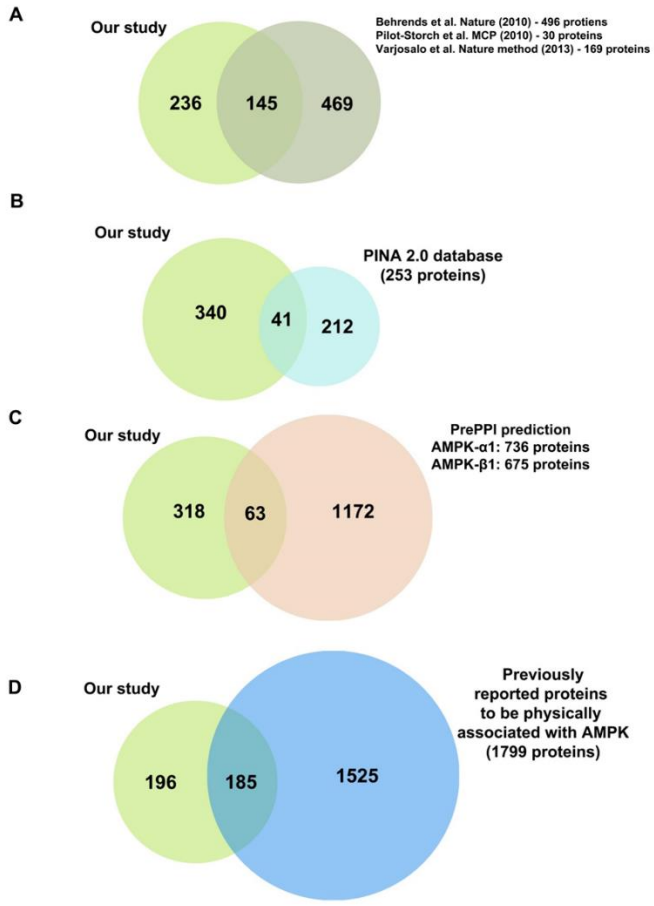

Figure 21. Comparison of AMPK-α1 and-β1 interactome with previous studies

IPI accession numbers of identified proteins were converted to gene symbols. First, we compared our datasets with interactors from 3 studies, including information of human AMPK binders proteins (A). The number of proteins from each paper is displayed. Second, we compared our datasets with the PINA 2.0 database (http://cbg.garvanunsw.edu.au/pina/) (B). Two hundred fifty-three proteins were extracted as AMPK-specific proteins from PINA 2.0 database. Third, we compared our datasets with putative AMPK-interacting proteins that were predicted using the PrePPI server (http://bhapp.c2b2.columbia.edu/PrePPI/) (C). Interaction prediction analysis using the PrePPI server yielded 736 and 675 proteins for AMPK-α1 and AMPK-β1, respectively. Finally, we summed the proteins from these approaches (A-C). A total of 1799 proteins were subjected to comparison analysis. Venn diagram of overlap (D) showing that 196 (51%) novel proteins were identified.

5.2. Relationship between AMPK and substrates in the AMPK -α1 and -β1 interactome

Because our baits are the catalytic and regulatory subunits of the AMPK complex, we expected some of its partners to be substrates for it. Thus, we determined whether the identified proteins were phosphorylated in tissues or cells and if their phosphorylation was AMPK-dependent. Our primary sources for this step were large phosphoproteome repositories, based on mass spectrometry, including the PhosphoSitePlus database[74], PHOSIDA database[75], and several phosphoproteomic studies in human, mouse, and rat[76-81]. Moreover, we predicted AMPK-dependent phosphorylation sites using GPS2.1[35] to examine the connections between the identified binding partners and AMPK.

As shown in Figure 22A, more than 92% of identified proteins were phosphorylated, over 78% of which (299 proteins) were predicted to be AMPK-dependently phosphorylated, using GPS2.1 with moderate confidence (Figure 22B). Further, of 1410 phosphorylation sites in the 299 proteins, 454 sites in 169 proteins were identified in earlier MS-based phosphoproteome studies (Figure 22C). Detailed information on the prediction analysis using GPS2.1 is shown in Figure 22D. For AMPK -α1 and -β1, nearly 80% of interactors were predicted to have phosphorylation sites with medium confidence (Figure 22D).

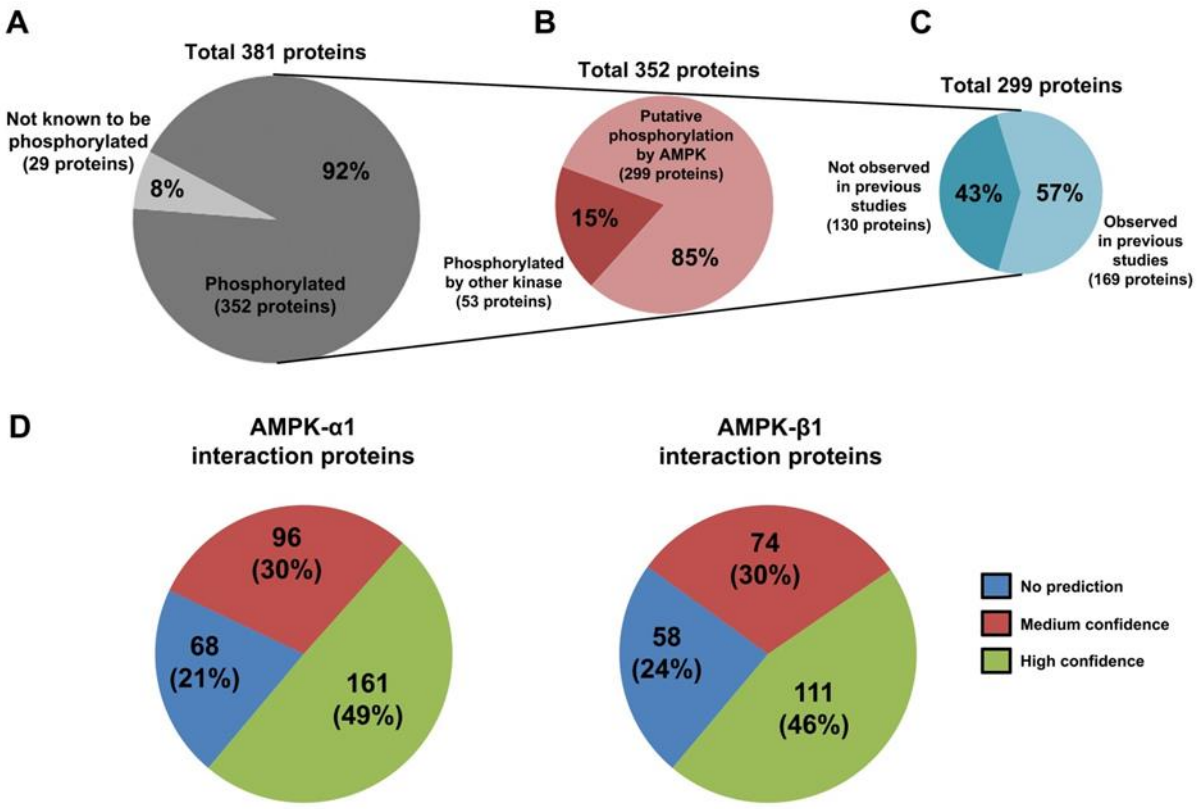

Figure 22. Relationship between AMPK and interacting proteins.

(A) In our AMPK interactome, 352 (92%) of 381 proteins were known phosphoproteins. (B) Prediction using GPS2.1 showed that 85% (299 proteins) of interacting proteins that are known as phosphoproteins were phosphorylated by AMPK. (C) Further, 169 (454 sites) of 299 predicted AMPK-dependent phosphoproteins (1410 phosphorylation sites) were detected from previous proteomics studies based on mass spectrometry; the remaining 130 phosphoproteins have not been reported. (D) Detailed information on the prediction analysis using GPS2.1. Percentage of predicted proteins with high confidence is shown in green. Percentage of predicted proteins with moderate confidence is displayed in red. Blue indicates percentage of proteins that are not predicted to be phosphoproteins. Approximately 80% of total proteins were predicted to be AMPK-dependently phosphorylated using GPS2.1 with moderate confidence.

Considering proteins that have been reported to associate with or be linked functionally to AMPK, our comparison analysis suggests that 92% (349/381) of identified proteins are related to AMPK, corroborating the functional correlation of these proteins with AMPK and validating the reliability of our approach for discovering novel AMPK interaction partners.

5.3. Regulation of actin cytoskeletal organization

We screened the AMPK-α1 and -β1 interactomes through functional grouping, based on their affiliation, and sorted AMPK interactors that were derived from pancreatic beta-cells. Most AMPK-α1- and -β1-binding proteins in the INS-1-specific group regulated actin cytoskeletal organization. Because a principal function of pancreatic beta-cells is to secrete hormones on stimulation, such as insulin through actin cytoskeleton remodeling[62,82], the proteins that are associated with the stimulus could be upregulated or activated in beta-cells versus other cell types, which might explain the GO analysis results.

Our bioinformatics analysis and literature search revealed that 16 proteins are linked to the regulation of actin cytoskeletal organization (Table 4)—Myh9, Myh10, Myh14, and Myl12b are associated with myosin class II (myosin II) activation and, as actin-binding proteins, are thus central in cell adhesion, migration, and division[51]. Myh9, Myh10, and Myh14 are 3 members of nonmuscle myosin II (NMII), including NMIIA, NMIIB, and NMIIC. Whereas Myh10 and Myh14 form complexes with AMPK in human cells[52,53], our AP-MS and co-IP data constitute novel findings of a link between AMPK and Myh9. Recent studies have suggested that NMII modulates GSIS through actin and focal adhesion remodeling in pancreatic beta-cells[54]. Further, AMPK regulates cell morphology and secretion by phosphorylating Myhl12b (known as MRLC)[19,55]. Although AMPK controls myosin II directly[56,57] and indirectly[19,58] in pancreatic beta-cells, role of AMPK in regulation of myosin remain unresolved. Our data support a model in which AMPK mediates myosin II-associated beta-cell functions, including the regulation of GSIS.

Notably, several proteins (IQGAP1, gelsolin, cofilin, Rac1, and RhoA) are related to reorganization and remodeling of filamentous actin (F-actin)[82], which regulates insulin secretion in beta-cells[82]. As scaffolding proteins and F-actin-binding protiens, IQGAP1 and gelsolin regulate cytoskeletal reorganization[59] and are also linked to pancreatic beta-cell functions, such as insulin secretion[60-62], beta-cell development[63,64], and cell-cell communication[61,65]. Whereas gelsolin interacts with AMPK-β in human cells[21], we report a novel interaction between AMPK and IQGAP1. Both proteins were confirmed to interact with AMPK-α1 and -β1 by co-IP and western blot (Figure 18B).

Cofilin-1 and Cofilin-2 are associated with glucose homeostasis, regulating insulin-stimulated GLUT4 translocation in muscle cells[69] and pancreatic beta-cells[70]. Rac1 is a member of the Rho family of GTPases, which govern cytoskeletal organization[83]. Recent evidence also implicates an association between AMPK and Rac1 in insulin secretion by pancreatic beta-cells[82,83]. RhoA is a small GTPase that regulates the actin cytoskeleton during the formation of stress fibers and is phosphorylated by AMPK[84]. Interestingly, RhoA controls several beta cell functions including beta-cell spreading and actin cytoskeleton dynamics through the Rho-ROCK pathway[85].

Because most of the direct interactions between AMPK and regulators of actin reorganization have not been reported in pancreatic beta-cells, our interactome is a resource that can be used to examine novel functions AMPK in regulating actin remodeling in pancreatic beta-cells. Further, the validation of 5 proteins (Gsn, Iqgap1, Myh9, Rhoa, and Rac1) should help us determine the function of AMPK-actin cytoskeleton assembly in regulating GSIS.

In conclusion, with the limitation of our pulldown approach using recombinant AMPK subunits expressed from a heterogeneous system, we performed a newly designed control experiment (Figure 4). To verify the reliability of the species affiliation (rat or human origin) analysis in the pulldown approach, all proteins that were considered to have originated from HEK293T cells (human origin) were analyzed by LC-MS/MS in the bait production stage, avoiding contact with proteins from INS-1 cells. Thus, fewer proteins were identified as Rat_only in the control experiments, compared to other pulldown experiments, indicating that this method can distinguish interactors of myc-AMPK-α1 and AMPK-β1

between INS-1 and human HEK293T cells (Figure 19). Further, BLAST analysis was performed to avoid missed interactions in the pulldown experiment. Only proteins with sequence identities of at least 99% were included in the final interactome of proteins that were identified in both the Rat_Human_Concurrently and Human_only groups. Lastly, we performed several additional experiments: direct IP in INS-1 cells to identify true positive interactors of rat origin, 4 biological replicates to improve the statistical significance, and statistical validation (SAINT analysis) to increase the credibility of our AP-MS data set versus the original experiment.

VI. CONCLUSION

Previous large-scale AP-MS studies analyzed 20~30 proteins for validation, using a tagging and overexpression system of baits and preys in HEK293T or other cells. However, due to the low transfection efficiency of INS-1 cells, we could not perform validation experiments based on an overexpression system. Thus, we performed several new experiments to improve the credibility and decrease the false positive selection as described below. A control pulldown experiment (HEK293T) and direct IP was newly performed to minimize false positives in the interactome by pulldown assay. The HEK293T control experiment in our pulldown approach showed that the species affiliation analysis can distinguish the origin of proteins that had been pulled down with myc-AMPK-α1 and AMPK-β1 (rat or human) (Figure 19).

Further, all experiments were repeated (4 biological replicates per bait), whereas the agarose datasets in the original submission were removed due to low reproducibility. The AP-MS data were processed using the SAINT algorithm instead of fold-changes to increase the reliability, as previous reports have demonstrated.

A total of 6 proteins that were related to actin remodeling, including 4 novel interactions (Iqgap1, Myh9, Rhoa, and Rac1), were validated by co-IP in INS-1, pancreatic beta cells. Consequently, we added several new experiments, refined the statistical analysis, and performed more validation

experiments to our data versus the original experiment. We stated that a total of 6 proteins, including previously validated proteins, were validated by immunoprecipitation in INS-1 cells.

In conclusion, we have identified many putative partners of AMPK-α1 and -β1 by combining affinity chromatography and mass spectrometry. With our stringent filtering criteria, our interactome comprised 325 and 243 proteins that interacted with AMPK-α1 and -β1, respectively. Our study confirms 185 previously described proteins and identifies 196 novel proteins that bind AMPK in our AMPK interactome datasets. Our data reinforce a model in which AMPK governs many functions that are linked to the regulation of actin organization. Specifically, several such proteins are closely associated with pancreatic beta-cell functions, including GSIS, beta-cell development, beta-cell differentiation, and cell-cell communication. Consequently, our interactome can be used to perform more detailed biochemical analyses of putative substrates and effectors of AMPK.

VII. References

1 Hwang, J. T., Kwon, D. Y. & Yoon, S. H. AMP-activated protein kinase: a potential target for the diseases prevention by natural occurring polyphenols. *New biotechnology* **26**, 17-22, doi:10.1016/j.nbt.2009.03.005 (2009).

2 Wong, A. K., Howie, J., Petrie, J. R. & Lang, C. C. AMP-activated protein kinase pathway: a potential therapeutic target in cardiometabolic disease. *Clinical science* **116**, 607-620, doi:10.1042/CS20080066 (2009).

3 Zhang, B. B., Zhou, G. & Li, C. AMPK: an emerging drug target for diabetes and the metabolic syndrome. *Cell metabolism* **9**, 407-416, doi:10.1016/j.cmet.2009.03.012 (2009).

4 Nagata, D. & Hirata, Y. The role of AMP-activated protein kinase in the cardiovascular system. *Hypertension research : official journal of the Japanese Society of Hypertension* **33**, 22-28, doi:10.1038/hr.2009.187 (2010).

5 Lage, R., Dieguez, C., Vidal-Puig, A. & Lopez, M. AMPK: a metabolic gauge regulating whole-body energy homeostasis. *Trends in molecular medicine* **14**, 539-549, doi:10.1016/j.molmed.2008.09.007 (2008).

6 Oakhill, J. S. *et al.* beta-Subunit myristoylation is the gatekeeper for initiating metabolic stress sensing by AMP-activated protein kinase (AMPK). *Proceedings of the National Academy of Sciences of the United States of America* **107**, 19237-19241, doi:10.1073/pnas.1009705107 (2010).

7 Hardie, D. G., Salt, I. P., Hawley, S. A. & Davies, S. P. AMP-activated protein kinase: an ultrasensitive system for monitoring cellular energy charge. *The Biochemical journal* **338 (Pt 3)**, 717-722 (1999).

8 Hawley, S. A. *et al.* Calmodulin-dependent protein kinase kinase-beta is an alternative upstream kinase for AMP-activated protein kinase. *Cell metabolism* **2**, 9-19, doi:10.1016/j.cmet.2005.05.009 (2005).

9 Sanders, M. J., Grondin, P. O., Hegarty, B. D., Snowden, M. A. & Carling, D. Investigating the mechanism for AMP activation of the AMP-activated protein kinase cascade. *The Biochemical journal* **403**, 139-148, doi:10.1042/BJ20061520 (2007).

10 Witters, L. A. & Kemp, B. E. Insulin activation of acetyl-CoA carboxylase accompanied by inhibition of the 5'-AMP-activated protein kinase. *The Journal of biological chemistry* **267**, 2864-2867 (1992).

11 Gwinn, D. M. *et al.* AMPK phosphorylation of raptor mediates a metabolic checkpoint. *Molecular cell* **30**, 214-226, doi:10.1016/j.molcel.2008.03.003 (2008).

12 Koo, S. H. *et al.* The CREB coactivator TORC2 is a key regulator of fasting glucose metabolism.

Nature **437**, 1109-1111, doi:10.1038/nature03967 (2005).

13 Kahn, B. B., Alquier, T., Carling, D. & Hardie, D. G. AMP-activated protein kinase: ancient energy gauge provides clues to modern understanding of metabolism. *Cell metabolism* **1**, 15-25, doi:10.1016/j.cmet.2004.12.003 (2005).

14 Fu, A., Eberhard, C. E. & Screaton, R. A. Role of AMPK in pancreatic beta cell function. *Molecular and cellular endocrinology* **366**, 127-134, doi:10.1016/j.mce.2012.06.020 (2013).

15 Sun, G. *et al.* Ablation of AMP-activated protein kinase alpha1 and alpha2 from mouse pancreatic beta cells and RIP2.Cre neurons suppresses insulin release in vivo. *Diabetologia* **53**, 924-936, doi:10.1007/s00125-010-1692-1 (2010).

16 Kim, W. H. *et al.* AICAR potentiates ROS production induced by chronic high glucose: roles of AMPK in pancreatic beta-cell apoptosis. *Cellular signalling* **19**, 791-805, doi:10.1016/j.cellsig.2006.10.004 (2007).

17 Ho, Y. *et al.* Systematic identification of protein complexes in Saccharomyces cerevisiae by mass spectrometry. *Nature* **415**, 180-183, doi:10.1038/415180a (2002).

18 Gingras, A. C., Gstaiger, M., Raught, B. & Aebersold, R. Analysis of protein complexes using mass spectrometry. *Nature reviews. Molecular cell biology* **8**, 645-654, doi:10.1038/nrm2208 (2007).

19 Banko, M. R. *et al.* Chemical genetic screen for AMPKalpha2 substrates uncovers a network of proteins involved in mitosis. *Molecular cell* **44**, 878-892, doi:10.1016/j.molcel.2011.11.005 (2011).

20 Kocher, T. & Superti-Furga, G. Mass spectrometry-based functional proteomics: from molecular machines to protein networks. *Nature methods* **4**, 807-815, doi:10.1038/nmeth1093 (2007).

21 Behrends, C., Sowa, M. E., Gygi, S. P. & Harper, J. W. Network organization of the human autophagy system. *Nature* **466**, 68-76, doi:10.1038/nature09204 (2010).

22 da Silva Xavier, G. *et al.* Role of AMP-activated protein kinase in the regulation by glucose of islet beta cell gene expression. *Proceedings of the National Academy of Sciences of the United States of America* **97**, 4023-4028 (2000).

23 Bertschinger, M., Schertenleib, A., Cevey, J., Hacker, D. L. & Wurm, F. M. The kinetics of polyethylenimine-mediated transfection in suspension cultures of Chinese hamster ovary cells. *Molecular biotechnology* **40**, 136-143, doi:10.1007/s12033-008-9069-0 (2008).

24 Reed, S. E., Staley, E. M., Mayginnes, J. P., Pintel, D. J. & Tullis, G. E. Transfection of mammalian cells using linear polyethylenimine is a simple and effective means of producing recombinant adeno-associated virus vectors. *Journal of virological methods* **138**, 85-98, doi:10.1016/j.jviromet.2006.07.024 (2006).

25 Rappsilber, J., Mann, M. & Ishihama, Y. Protocol for micro-purification, enrichment, pre-fractionation and storage of peptides for proteomics using StageTips. *Nature protocols* **2**, 1896-1906, doi:10.1038/nprot.2007.261 (2007).

26 Han, D. *et al.* Comprehensive phosphoproteome analysis of INS-1 pancreatic beta-cells using various digestion strategies coupled with liquid chromatography-tandem mass spectrometry. *Journal of proteome research* **11**, 2206-2223, doi:10.1021/pr200990b (2012).

27 Wisniewski, J. R., Zougman, A., Nagaraj, N. & Mann, M. Universal sample preparation method for proteome analysis. *Nature methods* **6**, 359-362, doi:10.1038/nmeth.1322 (2009).

28 Lundgren, D. H., Martinez, H., Wright, M. E. & Han, D. K. Protein identification using Sorcerer 2 and SEQUEST. *Current protocols in bioinformatics / editoral board, Andreas D. Baxevanis ... [et al.]* **Chapter 13**, Unit 13 13, doi:10.1002/0471250953.bi1303s28 (2009).

29 Choi, H. *et al.* SAINT: probabilistic scoring of affinity purification-mass spectrometry data. *Nature methods* **8**, 70-73, doi:10.1038/nmeth.1541 (2011).

30 Skarra, D. V. *et al.* Label-free quantitative proteomics and SAINT analysis enable interactome mapping for the human Ser/Thr protein phosphatase 5. *Proteomics* **11**, 1508-1516, doi:10.1002/pmic.201000770 (2011).

31 Scifo, E. *et al.* Drafting the CLN3 protein interactome in SH-SY5Y human neuroblastoma cells: a label-free quantitative proteomics approach. *Journal of proteome research* **12**, 2101-2115, doi:10.1021/pr301125k (2013).

32 Huang da, W., Sherman, B. T. & Lempicki, R. A. Systematic and integrative analysis of large gene lists using DAVID bioinformatics resources. *Nature protocols* **4**, 44-57, doi:10.1038/nprot.2008.211 (2009).

33 Franceschini, A. *et al.* STRING v9.1: protein-protein interaction networks, with increased coverage and integration. *Nucleic acids research* **41**, D808-815, doi:10.1093/nar/gks1094 (2013).

34 Saito, R. *et al.* A travel guide to Cytoscape plugins. *Nature methods* **9**, 1069-1076, doi:10.1038/nmeth.2212 (2012).

35 Xue, Y. *et al.* GPS 2.0, a tool to predict kinase-specific phosphorylation sites in hierarchy. *Molecular & cellular proteomics : MCP* **7**, 1598-1608, doi:10.1074/mcp.M700574-MCP200 (2008).

36 Buchse, T. *et al.* CIN85 interacting proteins in B cells-specific role for SHIP-1. *Molecular & cellular proteomics : MCP* **10**, M110 006239, doi:10.1074/mcp.M110.006239 (2011).

37 Sardiu, M. E. *et al.* Probabilistic assembly of human protein interaction networks from label-free quantitative proteomics. *Proceedings of the National Academy of Sciences of the United States of America* **105**, 1454-1459, doi:10.1073/pnas.0706983105 (2008).

38 Mosley, A. L. *et al.* Highly reproducible label free quantitative proteomic analysis of RNA polymerase complexes. *Molecular & cellular proteomics : MCP* **10**, M110 000687, doi:10.1074/mcp.M110.000687 (2011).

39 Lange, S., Sylvester, M., Schumann, M., Freund, C. & Krause, E. Identification of phosphorylation-dependent interaction partners of the adapter protein ADAP using quantitative mass spectrometry: SILAC vs (18)O-labeling. *Journal of proteome research* **9**,

4113-4122, doi:10.1021/pr1003054 (2010).

40 Green, A. S. *et al.* The LKB1/AMPK signaling pathway has tumor suppressor activity in acute myeloid leukemia through the repression of mTOR-dependent oncogenic mRNA translation. *Blood* **116**, 4262-4273, doi:10.1182/blood-2010-02-269837 (2010).

41 Li, Y. *et al.* AMPK phosphorylates and inhibits SREBP activity to attenuate hepatic steatosis and atherosclerosis in diet-induced insulin-resistant mice. *Cell metabolism* **13**, 376-388, doi:10.1016/j.cmet.2011.03.009 (2011).

42 Mihaylova, M. M. *et al.* Class IIa histone deacetylases are hormone-activated regulators of FOXO and mammalian glucose homeostasis. *Cell* **145**, 607-621, doi:10.1016/j.cell.2011.03.043 (2011).

43 Mendez, M. G., Kojima, S. & Goldman, R. D. Vimentin induces changes in cell shape, motility, and adhesion during the epithelial to mesenchymal transition. *FASEB journal : official publication of the Federation of American Societies for Experimental Biology* **24**, 1838-1851, doi:10.1096/fj.09-151639 (2010).

44 Sun, G. *et al.* LKB1 deletion with the RIP2.Cre transgene modifies pancreatic beta-cell morphology and enhances insulin secretion in vivo. *American journal of physiology. Endocrinology and metabolism* **298**, E1261-1273, doi:10.1152/ajpendo.00100.2010 (2010).

45 Tsuboi, T., da Silva Xavier, G., Leclerc, I. & Rutter, G. A. 5'-AMP-activated protein kinase controls insulin-containing secretory vesicle dynamics. *The Journal of biological chemistry* **278**, 52042-52051, doi:10.1074/jbc.M307800200 (2003).

46 Granot, Z. *et al.* LKB1 regulates pancreatic beta cell size, polarity, and function. *Cell metabolism* **10**, 296-308, doi:10.1016/j.cmet.2009.08.010 (2009).

47 Bae, H. B. *et al.* AMP-activated protein kinase enhances the phagocytic ability of macrophages and neutrophils. *FASEB journal : official publication of the Federation of American Societies for Experimental Biology* **25**, 4358-4368, doi:10.1096/fj.11-190587 (2011).

48 Kim, E. K. *et al.* Activation of AMP-activated protein kinase is essential for lysophosphatidic acid-induced cell migration in ovarian cancer cells. *The Journal of biological chemistry* **286**, 24036-24045, doi:10.1074/jbc.M110.209908 (2011).

49 Miranda, L. *et al.* AMP-activated protein kinase induces actin cytoskeleton reorganization in epithelial cells. *Biochemical and biophysical research communications* **396**, 656-661, doi:10.1016/j.bbrc.2010.04.151 (2010).

50 Bakalarski, C. E., Haas, W., Dephoure, N. E. & Gygi, S. P. The effects of mass accuracy, data acquisition speed, and search algorithm choice on peptide identification rates in phosphoproteomics. *Analytical and bioanalytical chemistry* **389**, 1409-1419, doi:10.1007/s00216-007-1563-x (2007).

51 Vicente-Manzanares, M., Ma, X., Adelstein, R. S. & Horwitz, A. R. Non-muscle myosin II takes centre stage in cell adhesion and migration. *Nature reviews. Molecular cell biology* **10**, 778-790, doi:10.1038/nrm2786 (2009).

52 Varjosalo, M. *et al.* Interlaboratory reproducibility of large-scale human protein-complex analysis by standardized AP-MS. *Nature methods* **10**, 307-314, doi:10.1038/nmeth.2400 (2013).

53 Ewing, R. M. *et al.* Large-scale mapping of human protein-protein interactions by mass spectrometry. *Molecular systems biology* **3**, 89, doi:10.1038/msb4100134 (2007).

54 Arous, C., Rondas, D. & Halban, P. A. Non-muscle myosin IIA is involved in focal adhesion and actin remodelling controlling glucose-stimulated insulin secretion. *Diabetologia* **56**, 792-802, doi:10.1007/s00125-012-2800-1 (2013).

55 Thaiparambil, J. T., Eggers, C. M. & Marcus, A. I. AMPK regulates mitotic spindle orientation through phosphorylation of myosin regulatory light chain. *Molecular and cellular biology* **32**, 3203-3217, doi:10.1128/MCB.00418-12 (2012).

56 Vazquez-Martin, A., Cufi, S., Oliveras-Ferraros, C. & Menendez, J. A. Polo-like kinase 1 directs the AMPK-mediated activation of myosin regulatory light chain at the cytokinetic cleavage furrow independently of energy balance. *Cell cycle* **11**, 2422-2426, doi:10.4161/cc.20438 (2012).

57 Lee, J. H. *et al.* Energy-dependent regulation of cell structure by AMP-activated protein kinase. *Nature* **447**, 1017-1020, doi:10.1038/nature05828 (2007).

58 Robitaille, A. M. & Hall, M. N. Ramping up mitosis: an AMPKalpha2-regulated signaling network promotes mitotic progression. *Molecular cell* **45**, 8-9, doi:10.1016/j.molcel.2011.12.018 (2012).

59 Malarkannan, S. *et al.* IQGAP1: a regulator of intracellular spacetime relativity. *Journal of immunology* **188**, 2057-2063, doi:10.4049/jimmunol.1102439 (2012).

60 Rittmeyer, E. N., Daniel, S., Hsu, S. C. & Osman, M. A. A dual role for IQGAP1 in regulating exocytosis. *Journal of cell science* **121**, 391-403, doi:10.1242/jcs.016881 (2008).

61 Kalwat, M. A., Wiseman, D. A., Luo, W., Wang, Z. & Thurmond, D. C. Gelsolin associates with the N terminus of syntaxin 4 to regulate insulin granule exocytosis. *Molecular endocrinology* **26**, 128-141, doi:10.1210/me.2011-1112 (2012).

62 Tomas, A., Yermen, B., Min, L., Pessin, J. E. & Halban, P. A. Regulation of pancreatic beta-cell insulin secretion by actin cytoskeleton remodelling: role of gelsolin and cooperation with the MAPK signalling pathway. *Journal of cell science* **119**, 2156-2167, doi:10.1242/jcs.02942 (2006).

63 Tekletsadik, Y. K., Sonn, R. & Osman, M. A. A conserved role of IQGAP1 in regulating TOR complex 1. *Journal of cell science* **125**, 2041-2052, doi:10.1242/jcs.098947 (2012).

64 Yermen, B., Tomas, A. & Halban, P. A. Pro-survival role of gelsolin in mouse beta-cells. *Diabetes* **56**, 80-87, doi:10.2337/db06-0769 (2007).

65 Hage, B., Meinel, K., Baum, I., Giehl, K. & Menke, A. Rac1 activation inhibits E-cadherin-mediated adherens junctions via binding to IQGAP1 in pancreatic carcinoma cells. *Cell communication and signaling : CCS* **7**, 23, doi:10.1186/1478-811X-7-23 (2009).

66 Fazal, F. *et al.* Essential role of cofilin-1 in regulating thrombin-induced RelA/p65 nuclear translocation and intercellular adhesion molecule 1 (ICAM-1) expression in endothelial cells. *The Journal of biological chemistry* **284**, 21047-21056, doi:10.1074/jbc.M109.016444 (2009).

67 Fanjul, M. *et al.* Evidence for epithelial-mesenchymal transition in adult human pancreatic exocrine cells. *The journal of histochemistry and cytochemistry : official journal of the Histochemistry Society* **58**, 807-823, doi:10.1369/jhc.2010.955807 (2010).

68 Spruill, W. A., Zysk, J. R., Tres, L. L. & Kierszenbaum, A. L. Calcium/calmodulin-dependent phosphorylation of vimentin in rat sertoli cells. *Proceedings of the National Academy of Sciences of the United States of America* **80**, 760-764 (1983).

69 Chiu, T. T., Patel, N., Shaw, A. E., Bamburg, J. R. & Klip, A. Arp2/3- and cofilin-coordinated actin dynamics is required for insulin-mediated GLUT4 translocation to the surface of muscle cells. *Molecular biology of the cell* **21**, 3529-3539, doi:10.1091/mbc.E10-04-0316 (2010).

70 Wang, Z., Oh, E., Clapp, D. W., Chernoff, J. & Thurmond, D. C. Inhibition or ablation of p21-activated kinase (PAK1) disrupts glucose homeostatic mechanisms in vivo. *The Journal of biological chemistry* **286**, 41359-41367, doi:10.1074/jbc.M111.291500 (2011).

71 Pilot-Storck, F. *et al.* Interactome mapping of the phosphatidylinositol 3-kinase-mammalian target of rapamycin pathway identifies deformed epidermal autoregulatory factor-1 as a new glycogen synthase kinase-3 interactor. *Molecular & cellular proteomics : MCP* **9**, 1578-1593, doi:10.1074/mcp.M900568-MCP200 (2010).

72 Wu, J. *et al.* Integrated network analysis platform for protein-protein interactions. *Nature methods* **6**, 75-77, doi:10.1038/nmeth.1282 (2009).

73 Zhang, Q. C., Petrey, D., Garzon, J. I., Deng, L. & Honig, B. PrePPI: a structure-informed database of protein-protein interactions. *Nucleic acids research* **41**, D828-833, doi:10.1093/nar/gks1231 (2013).

74 Hornbeck, P. V. *et al.* PhosphoSitePlus: a comprehensive resource for investigating the structure and function of experimentally determined post-translational modifications in man and mouse. *Nucleic acids research* **40**, D261-270, doi:10.1093/nar/gkr1122 (2012).

75 Gnad, F., Gunawardena, J. & Mann, M. PHOSIDA 2011: the posttranslational modification database. *Nucleic acids research* **39**, D253-260, doi:10.1093/nar/gkq1159 (2011).

76 Wisniewski, J. R., Nagaraj, N., Zougman, A., Gnad, F. & Mann, M. Brain phosphoproteome obtained by a FASP-based method reveals plasma membrane protein topology. *Journal of proteome research* **9**, 3280-3289, doi:10.1021/pr1002214 (2010).

77 Weintz, G. *et al.* The phosphoproteome of toll-like receptor-activated macrophages. *Molecular systems biology* **6**, 371, doi:10.1038/msb.2010.29 (2010).

78 Oppermann, F. S. *et al.* Large-scale proteomics analysis of the human kinome. *Molecular & cellular proteomics : MCP* **8**, 1751-1764, doi:10.1074/mcp.M800588-MCP200 (2009).

79 Daub, H. *et al.* Kinase-selective enrichment enables quantitative phosphoproteomics of the kinome across the cell cycle. *Molecular cell* **31**, 438-448, doi:10.1016/j.molcel.2008.07.007

(2008).

80 Olsen, J. V. *et al.* Global, in vivo, and site-specific phosphorylation dynamics in signaling networks. *Cell* **127**, 635-648, doi:10.1016/j.cell.2006.09.026 (2006).

81 Olsen, J. V. *et al.* Quantitative phosphoproteomics reveals widespread full phosphorylation site occupancy during mitosis. *Science signaling* **3**, ra3, doi:10.1126/scisignal.2000475 (2010).

82 Kalwat, M. A. & Thurmond, D. C. Signaling mechanisms of glucose-induced F-actin remodeling in pancreatic islet beta cells. *Experimental & molecular medicine* **45**, e37, doi:10.1038/emm.2013.73 (2013).

83 Li, J., Luo, R., Kowluru, A. & Li, G. Novel regulation by Rac1 of glucose- and forskolin-induced insulin secretion in INS-1 beta-cells. *American journal of physiology. Endocrinology and metabolism* **286**, E818-827, doi:10.1152/ajpendo.00307.2003 (2004).

84 Gayard, M. *et al.* AMPK alpha 1-induced RhoA phosphorylation mediates vasoprotective effect of estradiol. *Arteriosclerosis, thrombosis, and vascular biology* **31**, 2634-2642, doi:10.1161/ATVBAHA.111.228304 (2011).

85 Hammar, E., Tomas, A., Bosco, D. & Halban, P. A. Role of the Rho-ROCK (Rho-associated kinase) signaling pathway in the regulation of pancreatic beta-cell function. *Endocrinology* **150**, 2072-2079, doi:10.1210/en.2008-1135 (2009).

Abstract in Korean

초 록

서론: Heterotrimeric 효소 단백질으로써, AMP-activated protein kinase (AMPK) 는 세포 내 에너지 항상성 조절에 있어 주요한 물질대사 감지기능을 하고, 여러 조직에서 발현된다. 특히, AMPK 는 제 2형 당뇨와 연관된 인슐린 저항성에 기여한다. 일반적으로, 세포 내 process 는 단백질 인산화효소의 밀접한 제어를 필요로 하는데, 이는 인산화효소의 다른 기질들과의 complex 형성을 통해 영향을 받는다. 이러한 조절 기능과 발병기전에 중대한 역할에도 불구하고, 단백질 인산화효소들의 결합 단백질에는 제한된 연구가 진행되어있다.

방법: AMPK 결합 단백질을 동정하기 위해, AMPK-α1 과 -β1 subunit 을 대상으로 대규모의 affinity purification (AP)-mass spectrometry (MS) 분석을 수행하였다. AP-MS 수행 전에, 6-myc tagged AMPKα1/β1 재조합 단백질들을 INS-1 세포에 일시적으로 transfection 하였다. Immunoprecipitation 은 2개의 다른 bead (anti-myc antibody-conjugated agarose 와 magnetic beads) 를 동반하여 수행하였다. In-gel trypsin digestion 과정 후, 해당 펩타이드들을 LC-MS/MS 3-반복 분석을 진행하였다.

결과: AP-MS 접근을 이용한 대규모 AMPKα1/β1 interactomes 분석을 통하여, 381개의 unique 단백질들 (325개 AMPK-α1 와 243개 AMPK-β1 interactors) 을 동정하였다.

Agarose bead 를 사용한 IP 보다 magnetic bead 를 사용한 경우 더 많은 수의 결합 단백질들이 동정되었다. 또한, 현존하는 단백질−단백질 결합 데이터베이스 상에 아직 알려져 있지 않은 196개 새로운 interactors 를 동정하였다. 특히, 생물정보학적 분석에 있어, 새로운 interactors 들은 액틴 세포골격 (actin cytoskeleton) 조절에 관련된 기능을 중재하고 있었다. 구체적으로, 몇 단백질들은 베타 세포 발달, 베타 세포 분화, 포도당 자극 인슐린 분비 (glucose-stimulated insulin secretion, GSIS), 세포−세포간 communication 등을 포함한 췌장 베타 세포 기능에 연계되어 있었다.

결론: 이러한 AMPK-특이적 interactome 분석은 AMPK 의 생물정보학적 기능 연구에 기여할 수 있고, 새로운 interactors 는 췌장 베타 세포 기능과 관련하여, AMPK 신호 전달 과정 연구에서 귀중한 타겟이 될 것이다.

* 본 내용은 *Scientific Reports* 학술지에 출판 완료된 내용임

주요어: AMP-activated protein kinase (AMPK), affinity purification (AP)-mass spectrometry (MS), 췌장 베타 세포, interactome, 단백질체학

학 번: 2009-21863